MINISTRY OF TECHNOLOGY

AERONAUTICAL RESEARCH COUNCIL
REPORTS AND MEMORANDA

Measurement of the Moments and Product of Inertia of the Fairey Delta 2 Aircraft

By C. S. BARNES and A. A. WOODFIELD
Aerodynamics Dept., R.A.E., Bedford

Measurement of the Moments and Product of Inertia of the Fairey Delta 2 Aircraft

By C. S. BARNES and A. A. WOODFIELD

Aerodynamics Dept., R.A.E., Bedford

Summary.

The moments and product of inertia of the Fairey Delta 2 aircraft have been measured using the method of spring restrained oscillations. The moment of inertia results were satisfactory, but difficulty was found in determining the product of inertia due to unsatisfactory design of the single point suspension rig.

A dependence of roll period on roll amplitude was discovered and this may be due to some form of ground effect. The damping in roll was found to vary with fuel state.

The agreement between the manufacturer's estimates and the measured moments and product of inertia was poor, and there is clearly a continuing need for inertia measurements. Simple estimates of the fuel inertias compared well with the measured values, agreement being within the expected accuracy of the measurements. The fuel load of the Fairey Delta 2 is relatively small, and simple estimates for greater loads might be less satisfactory.

LIST OF CONTENTS

1. Introduction.

Much of the flying of research aircraft, such as the Fairey Delta 2, is devoted to dynamic tests designed to enable the measurement of aerodynamic stability derivatives for comparison with estimated derivatives or with derivatives measured in wind tunnels. Such comparisons are not of great value unless the moments of inertia used in the dynamic equations of motion are known to at least the same accuracy as that of the various measurements necessary for the extraction of stability derivatives from flight results. It is desirable to know the moments of inertia of a research aircraft to an accuracy of about 1 per cent and, for a moderately slender aircraft such as the Fairey Delta 2, the inclination of the principal axis needs to be known to about 0·1°.

At present, techniques for estimating the moments of inertia of an aircraft are not sufficiently accurate and direct measurements must be made in ground tests. Of the variety of possible methods[1], the technique of mounting the aircraft on knife edges and constraining it to perform spring restrained oscillations is relatively simple and lends itself particularly well to the measurement of the inertia in roll and pitch. Earlier tests at R.A.E. Bedford[2,3,4] have used this method with success and it has been used for these tests on the Fairey Delta 2.

The measurement of the moment of inertia in yaw, and the product of inertia, is more difficult. Simple rigs cannot restrict the degrees of freedom of the oscillating motion to one only. This problem was experienced with the Avro 707B aircraft[3] which was oscillated about a single point suspension. The test method used[5] relied on the coupling induced between the roll and yaw motion when an aircraft is oscillated in the yaw mode about an axis other than the principal yawing inertia axis. The tests should have enabled both the yawing moment of inertia and the product of inertia to be determined but were complicated by severe interference from rocking and pendulum or swaying modes associated with the suspension rig.

A single point suspension rig for the Fairey Delta 2 was designed before the Avro 707B tests were made. Some steps were taken after these tests to reduce the interference then anticipated on the Fairey Delta 2 rig. Two sets of springs and three pairs of fore and aft spring attachment positions were provided and the combination leading to least interference was selected. A method of analysis was also developed to enable the product of inertia to be extracted in spite of the interference and to minimise this problem by suitable design of future rigs[6].

The roll inertia tests on the Fairey Delta 2 revealed a phenomenon which is believed not to have been found during any previous inertia measurements. The period of the rolling oscillation was found to increase with oscillation amplitude. Various explanations were sought, including an investigation of fuel sloshing by oscillating a separate set of Fairey Delta 2 wings, without coming to a definite conclusion.

The virtual inertia, due to oscillating the aircraft in air rather than in a vacuum, was estimated using the data of Malvestuto and Gale[7]. These data, which were derived for aircraft having straight wings of fairly high aspect ratio, were not representative of the Fairey Delta 2, which has a delta wing with 59·9° leading edge sweep and an aspect ratio of two (*see* Table 1 and Fig. 1). However, experience with inertia measurements on a model of the Handley Page HP 115 aircraft[4] suggested that extrapolation was justified.

Estimates were made of the additional inertia due to fuel using the data of Refs. 8 and 9.

2. Test Methods and Analysis.

Prior to the moment of inertia measurements, the position of the centre of gravity of the aircraft was determined to enable the measured inertias to be referred to the correct axis.

The inertia measuring technique used in roll and pitch was identical to that of earlier tests at R.A.E. Bedford[2,3,4]. The aircraft was mounted on knife edges and was constrained, by means of springs, to oscillate about axes parallel to the aircraft pitching and fuselage longitudinal datum axes respectively. In yaw the aircraft was suspended by a single cable in a similar manner to the Avro 707B[3] and was constrained by springs to perform yawing oscillations with some roll coupling. All tests, except the centre of gravity determination, were done with the undercarriage retracted, the flight test configuration.

The spring rates were chosen, using the manufacturer's inertia estimates, to give oscillation periods representative of those of the flight longitudinal short period and Dutch roll oscillations.

Additional tests were made on rolling oscillations of the aircraft wings alone, to investigate the effect

of fuel sloshing. The wings were constrained in a manner similar to that for the rolling oscillations of the complete aircraft.

The motion of the aircraft was sensed by rate gyroscopes. In pitch and roll a single gyroscope was used, orientated to sense the oscillations about the appropriate axis, with a measuring range of $\pm 2\frac{1}{2}°$/sec. In yaw the technique required two rate gyroscopes, both with a range of $\pm 2\frac{1}{2}°$/sec, orientated about the yawing and rolling axes. The rate gyroscope was calibrated over $\pm 10°$/sec for the rolling oscillations of the wings alone.

The reference time base for measuring the period of the oscillations was provided by a 50 Hz tuning fork calibrated at the National Physical Laboratory. The outputs from the tuning fork, and from the rate gyroscopes, were recorded using a continuous trace galvanometer recorder.

2.1. *Measurement of the Centre of Gravity Position.*

Inspection of Fig. 2 shows that the relation:

$$(R_N + R_M)(\bar{x}\cos\theta + \bar{z}\sin\theta) + R_N(d_2 - d_1) - R_M d_1 = 0 \qquad (1)$$

where d_1 = distance of the mainwheel reaction behind the cg datum

d_2 = distance between the nosewheel and mainwheel reactions

R_M = total mainwheel reaction

R_N = nosewheel reaction

$\bar{x}$ = distance of aircraft centre of gravity aft of cg datum

$\bar{z}$ = height of aircraft centre of gravity above cg datum

θ = aircraft pitch attitude

holds for pitching moments about the centre of gravity datum.

Equation (1) may be rearranged as:

$$\{d_1 - d_2 R_N/(R_N + R_M)\}\sec\theta = \bar{x} + \bar{z}\tan\theta. \qquad (2)$$

The value of the left hand side of the equation can be determined from measured quantities, and plotting it against $\tan\theta$ for various pitch attitudes, yields $\bar{x}$ and $\bar{z}$. The aircraft weight is given by $R_M + R_N$.

The aircraft was weighed with its mainwheels and nosewheel on separate weighbridges, and its pitch attitude was changed, over the range $-5°$ to $+8°$, by varying the height of the nosewheel weighbridge. An inclinometer on the aircraft datum bar was used to measure the aircraft attitude.

Except for the lowered undercarriage, the tests were made in the normal flight condition of the aircraft, a dummy pilot weighing 180 lb being included. Tests were made with the aircraft nominally empty, half fuelled and fully fuelled. A small quantity of fuel, approximately 110 lb, which could not be drained, remained in the aircraft wings during the aircraft-nominally-empty test.

A correction, due to undercarriage retraction, to the measured centre of gravity position, was calculated from the known weight and geometry of the undercarriage. The effect, on the aircraft centre of gravity position of the change of oleo extension with aircraft attitude during the tests was negligible.

2.2. *Measurement of the Moment of Inertia in Roll.*

2.2.1. *The complete aircraft.* The system employed was similar to that used in earlier tests at R.A.E.[3] and is shown in Fig. 3. The aircraft was mounted on a cradle supported on two knife edges approximately symmetrically disposed fore and aft about the aircraft centre of gravity. Cages containing four vertical coil springs of measured total rate were attached to the wing jacking points. The aircraft was thus constrained to oscillate about an axis through the knife edges, parallel to the fuselage longitudinal

4

datum axis. A useful check on the accuracy of the results was made by placing a tray containing seven 56 lb weights on the wing upper surface close to each wing tip. The additional inertia due to the weights could be accurately calculated and compared with the measured additional inertia.

The total moment of inertia, $A_{K.E.}$, of the system about an axis through the knife edges is given by:

$$A_{K.E.} = (P_x/2\pi)^2 (\lambda_x y_s^2 - W_T \bar{z}_T) \tag{3}$$

derived in the Appendix where

P_x = roll oscillation period

W_T = total oscillating weight

y_s = distance of springs outboard of the knife edges

$\bar{z}_T$ = height of system centre of gravity above knife edges

λ_x = combined stiffness of springs

The weight W_T includes 1/3 of the spring weight as a correction for heavy springs.

The rolling oscillation was excited by displacing one wing tip through a nominal amplitude of $\pm \frac{1}{2}, \frac{3}{4}$ or 1 in, where 1 in is equivalent to an angular displacement of 0·37°. Tests were made with the aircraft containing no fuel (nominal), half fuel and full fuel.

2.2.2. Period and damping in roll of the aircraft wings. In order to investigate the effect of fuel sloshing on aircraft oscillations, a rig was constructed upon which the Fairey Delta 2 wings alone, which contain about 83 per cent of the total fuel, could be oscillated in roll. The rig is shown in Fig. 4. The roll axis was in the same position relative to the wings as that used for the aircraft rolling inertia measurements but was 3·8 ft above the ground compared with 2·2 ft for the complete aircraft. The wings were constrained to roll about this axis in a similar manner to that in the complete aircraft tests.

Weights were placed on both wing tips to increase the system inertia so that using the same restraining springs, the period of the rolling oscillation was close to that of the complete aircraft for the nominally empty fuel state. These weights were left on the wings for the duration of the tests.

The geometry of the wing tanks is shown in Fig. 7; tests were made at the fuel states shown in Table 2. Fuel states 2, 4 and 9 correspond to the aircraft fuel states of nominally empty, half fuel and full fuel respectively, excluding the collector tank in the aircraft fuselage. This tank was not included in the wings ·rig but on the complete aircraft contained 59 gal for the full fuel and 53 gal for the half fuel condition. Tests were made over a range of amplitude from $\pm \frac{1}{4}$ in to ± 4 in measured at the wing tip, where 1 in is again equivalent to an angular displacement of 0·37°.

An equation similar in form to equation (3) relates the moment of inertia of the wings rig about the rolling axis to the period of the oscillations. Since the actual inertia of the Fairey Delta 2 wings is of little fundamental interest, and since the height of the centre of gravity of the rig above the knife edges would be difficult to determine, the measured value of the oscillation period may be taken as an indication of the effects of fuel state and roll amplitude upon inertia measurement. Of more fundamental interest is the effect of fuel state on the damping of the oscillation.

2.3. Measurement of the Moment of Inertia in Pitch. The system was very similar to that of earlier tests at R.A.E.[2,3,4] and is shown in Fig. 5. The aircraft was supported on knife edges at the two rear jacking points, with its nose resting in a cradle attached to the nose jacking bar. The cradle was suspended from six vertical coil springs of known rates. The aircraft was thus constrained to oscillate about an axis through the two knife edges, parallel to the aircraft pitching axis.

Provision was made for attaching four 56 lb weights beneath the nose cradle. As in the roll case, comparison between the calculated and measured inertia of the weights gave a check on the experimental accuracy.

5

It is shown in the Appendix that the total moment of inertia, $B_{K.E.}$, of the system about an axis through the knife edges is given by:

$$B_{K.E.} = (P_y/2\pi)^2 (\lambda_y x_s^2 - W_T \bar{z}_T) \qquad (4)$$

in a form similar to equation (3).

The pitching oscillation was excited by pushing downwards on the aircraft nose forward of the nose support. Tests were made with nominal oscillation amplitudes of $\pm\frac{1}{4}, \frac{1}{2}, \frac{3}{4}$ and 1 in at the nose-boom tip (where 1 in is equivalent to an angular displacement of $0.12°$) and with the aircraft containing no fuel (nominal), half fuel and full fuel.

2.4. Measurement of the Moment of Inertia in Yaw and the Product of Inertia.

As in an earlier test at R.A.E.[3], the aircraft was suspended, with its fuselage longitudinal datum axis horizontal, from a 20 ton Coles crane, as shown in Fig. 6. A trapezium shaped spreader frame, picking up on the two wing lifting points and on the nose jacking bar, was needed to prevent the transmission of unacceptable side loads to the pick-up points. The aircraft was restrained in yaw by two pairs of springs attached to cantilever brackets extending below the fuselage.

Such a system clearly allows the aircraft to rotate about all three axes and to translate along the pitch and roll axes, whilst restrained by the springs. Woodfield[6] has shown that three lateral oscillatory modes will in general be excited by a lateral input, unless the rig is suitably designed to prevent the excitation of two of these modes. No longitudinal motion will be excited providing that the initial input has no longitudinal component.

The three lateral modes of the system are:

(i) *The yaw mode.* This consists mainly of yawing motion but with some coupled roll motion and a negligible amount of sideways translation. There is normally roll/yaw coupling since the rolling moment due to the restraining springs is not in general equal and opposite to that caused by the system (the aircraft plus suspension rig) not being oscillated about its principal yawing inertia axis. The particular condition when the two rolling moments do cancel is that utilised in the analysis technique of Boucher et al[5].

(ii) *The rocking mode.* This is mainly a rolling motion but with some associated lateral translation and a very small amount of yaw.

(iii) *The swaying mode.* This is mainly an oscillatory sideways translation but with some coupled roll motion and a negligible amount of yaw.

Interference from both the rocking mode and the swaying mode was present during the earlier tests on the Avro 707B aircraft[3] and during the tests on the Fairey Delta 2. At the time of the design of the rigs for these tests, criteria for minimising interference were not known. The positions of the spring attachment brackets, fore and aft of the aircraft centre of gravity, and the spring rates were chosen such that during yawing oscillations, no resultant side force would be exerted on the aircraft by the springs. However, the bracket cantilever stiffness, which varied with the height of the spring attachment position, significantly modified the effective spring stiffness and introduced a resultant side force during the yawing oscillations, thus aggravating the interference problem. This side force due to yaw, and the related yawing moment due to lateral translation, is expressed in the equations of motion of the system, discussed later, by the term:

$$\Delta(\lambda_i x_i) = \lambda_F x_F - \lambda_R x_R \qquad (5)$$

where x_F = distance of front springs ahead of the yaw suspension axis

x_i = general yaw spring distance ahead of the yaw suspension axis

x_R = distance of rear springs aft of the yaw suspension axis

λ_F = combined effective stiffness of front yaw springs

λ_i = general effective yaw spring pair stiffness

λ_R = combined effective stiffness of rear yaw springs

6

The spring pair stiffnesses are corrected for support bracket cantilever stiffness.

Physically the expression in equation (5) is the resultant spring side force due to unit rotation in yaw.

2.4.1. *Moment of inertia.* The moment of inertia in yaw, C_T, of the complete system, about the yawing axis through the system centre of gravity, is shown in the Appendix to be given by:

$$C_T = (P_z/2\pi)^2 (\lambda_F x_F^2 + \lambda_R x_R^2) \tag{6}$$

where P_z is the period of the system yaw mode.

Equation (6) strictly applies only when there is no roll motion in the yaw mode, and there is no resultant spring side force[5,6]. Due to the interference from the rig modes it was not possible during the tests to determine when there was no roll motion present in the yaw mode. Also, due to the finite cantilever stiffness of the spring support brackets, there was a resultant spring side force during the yawing oscillations. A small correction for the additional terms introduced into equation (6) by the small amount of roll motion in the yaw mode, and by the resultant spring side force, could be applied[6] as described in the Appendix.

2.4.2. *Product of inertia.* The method described by Boucher et al[5] for determining the product of inertia depends on determining the rig conditions for which the roll/yaw ratio of the system yaw mode is zero. The relative vertical position of the front and rear spring pairs is adjusted to eliminate any roll motion. The product of inertia E is then given by

$$E = \Delta(\lambda_i x_i z_i)/\omega_1^2 \tag{7}$$

where ω_1 is the natural frequency of the system yaw mode and z_i is the distance of the general spring attachment point below the system centre of gravity. The Δ notation signifies the difference between the total values of $\lambda_i x_i z_i$ for the front and rear spring pairs, in a similar manner to $\Delta(\lambda_i x_i)$ in equation (5).

It may be shown[6] that equation (7) is only true when a further condition, in addition to zero roll/yaw ratio of the yaw mode, applies. This is that the product of $\Delta(\lambda_i x_i)$, the resultant spring side force due to unit rotation in yaw, and the parameter $\{W_T h/q - \Sigma(\lambda_i z_i)\}$ should be zero, where h and q are rig geometry parameters shown in Fig. 21, and Σ means the sum of the general products $\lambda_i z_i$. This further condition eliminates the interference from unwanted lateral modes in the analysis.

The Fairey Delta 2 rig was designed for use with Boucher's method before the tests on the Avro 707B aircraft[3] were made. The interference from the system rocking and swaying modes found then, was also experienced with the Fairey Delta 2 rig, although it was anticipated and reduced somewhat by providing three pairs of spring attachment positions and two sets of springs. Preliminary tests showed that the interference from the unwanted modes appeared to be least for the stiffer set of springs attached at the longitudinal positions furthest from the centre of gravity and this configuration was adopted for the main series of tests. However, the effect of the cantilever stiffness of the spring attachment brackets modified the spring stiffnesses sufficiently to introduce a significant resultant spring force and it was this that led to most of the interference problems.

It was found experimentally that the interference was also reduced by careful choice of the method of exciting the yawing motion. A $\frac{1}{2}$-cosine input involving pressing on the aircraft nose in phase with the motion during half the cycle appeared to be best, and it was afterwards shown theoretically[6] that this input was preferable to a step input.

Woodfield developed his analysis specifically for use with the Fairey Delta 2 results and at the same time to provide criteria for future rig designs. Using his method, it can be shown that the product of inertia may be related to the roll/yaw ratio, ϕ/ψ, of the system yaw mode, and to the natural frequencies ω_1, ω_2 and ω_3 of the yaw, rocking and swaying modes respectively, by the expression

$$E + \frac{\phi}{\psi}\left[A_T \left(\frac{\omega_2}{\omega_1}\right)^2 - \frac{\{W_T h/q - \Sigma(\lambda_i z_i)\}^2}{W_T (\omega_3^2 - \omega_1^2)\omega_1^2/g} - A_T \right] = \left[\frac{\Delta(\lambda_i x_i z_i)}{\omega_1^2} + \frac{\Delta(\lambda_i x_i)\{W_T h/q - \Sigma(\lambda_i z_i)\}}{W_T (\omega_3^2 - \omega_1^2)\omega_1^2/g} \right] \tag{8}$$

7

where A_T is the roll inertia of the system about a horizontal axis through the system centre of gravity. The importance of the product term mentioned above is clearly seen from equation (8). When this term and the roll/yaw ratio of the mode are zero, then equation (8) reduces to Boucher's expression for E, equation (7).

The roll/yaw ratio is derived using the technique[6] of plotting the peak values of the rate of roll against the concurrent values of the rate of yaw. The frequency ω_1 may be determined directly from the rate of yaw record of the oscillation since the interference from the unwanted modes on the true rate of yaw is negligible. The frequency ω_2 of the system rocking mode was measured directly by taking records with only the rocking mode excited. The frequency ω_3 of the system swaying mode was calculated using the expression:

$$\omega_3^2 = g(W_T/q + \Sigma\lambda_i)/W_T$$

from Ref. 6.

2.5. *Estimation of the Virtual Inertia.*

In general a body moving in a fluid disturbs fluid having inertia. The inertia of this fluid, the virtual inertia, must be subtracted from the measured moment of inertia to obtain the correct structural inertia. For flight test purposes, the virtual inertia appropriate to the correct aircraft altitude, and oscillation axis, must be included in the moment of inertia values used. There is now some experimental evidence that the values of the virtual moments of inertia obtained from oscillation tests in still air can be applied to flight conditions if factored by the relative density[10]. It was thus necessary to calculate virtual inertias about the system oscillation axis and also about axes through the aircraft centre of gravity, the latter for the range of test altitude required. The method used was that of Malvestuto and Gale[7]. As Fennell[4] points out. this method was derived for aircraft having wings of high aspect ratio with small taper. but his experience with the Handley Page HP 115 aircraft suggests that the data of Ref. 7 may be extrapolated with reasonable accuracy, although there is some doubt due to the affect of ground proximity on the virtual inertia.

It should be mentioned that there is also an analogous virtual mass but this was found to be negligible.

3. *Results.*

3.1. *Aircraft Centre of Gravity Position.*

The plots of equation (2) are shown in Fig. 8. The results for all three fuel states adequately define straight lines. However, the slope of the best straight line through the results for the half fuel state, implies a centre of gravity height totally incompatible with the heights for the nominally empty and full fuel conditions when related to the quantity of fuel added. This is believed to be due to fuel movement as the aircraft attitude was changed during the test.

For the half fuel condition, the points at positive aircraft attitude alone appeared to define another straight line, and it was considered that, as positive attitude is more representative of the aircraft in flight, it was valid to use only these points to determine the centre of gravity position. A centre of gravity height compatible with those for the empty and full fuel conditions was then obtained. The centre of gravity height is significant mainly in the axis transfer term in roll and it will be seen later, Section 3.2, that the roll results for the half fuel case are unreliable. It was not, therefore, considered worthwhile to correct for the effects of fuel movement, since quite elaborate calculations would have been necessary.

The derived centre of gravity positions relative to the centre of gravity datum are shown in Table 3. The cg datum is 240 in ahead of the wing trailing edge and 14·4 in below the fuselage longitudinal datum axis. Raising the undercarriage is seen to shift the centre of gravity forward by rather more than 1 in and to raise it by rather more than 2 in, depending on fuel state.

It is estimated that the longitudinal centre of gravity position is accurate to $\pm 0\cdot1$ in and the vertical position to $\pm 0\cdot5$ in for the empty and full fuel states. The results for half fuel are thought to be slightly less accurate.

8

3.2. *Moment of Inertia in Roll.*

Fig. 9 shows plots of the period of the roll oscillation, P_x, to a very large scale, *versus* oscillation amplitude, expressed as the angle of roll ϕ. It is seen that for the nominally empty and full aircraft, the period increases with increasing oscillation amplitude, implying that if equation (3) applies, then the system inertia (including the virtual inertia and fuel inertia) or the spring stiffness varies with oscillation amplitude. The recorded roll rate trace was closely sinusoidal, showing that no significant non-linear terms were omitted in the derivation of equation (3). No trend can be drawn from the half fuel state, the results from which show considerable scatter. For the nominally empty and full aircraft the variation of period with amplitude appears to be approximately linear.

Corresponding plots for the roll period of the aircraft wings alone are shown in Fig. 10. The fuel states illustrated are those of the complete aircraft tests, plus the test with the aircraft wings completely empty of fuel. The linear increase of roll period with roll amplitude is again present, but at a much reduced rate; a larger range of roll amplitude was investigated than for the complete aircraft. The results for the fuel states not shown exhibit large scatter, similar to the half fuel case (fuel state 4), presumably due to fuel sloshing.

Those results from both the complete aircraft and the wings tests which were not too scattered due to fuel sloshing in partially filled tanks, suggest that P_x increases linearly with ϕ. Even at the relatively large maximum values of roll amplitude for the wings alone, compared with the complete aircraft, the roll period is still increasing. It thus seems very likely that the true inertia is associated with a roll period corresponding to an oscillation of zero amplitude. This assumption was made when determining the value of P_x for use in equation (3). Possible causes of the variation of P_x with ϕ are discussed in Section 5. The method of least squares was used to fit the best straight lines through the experimental points for the complete aircraft, Fig. 9, and the intercept on the P_x axis was used in equation (3). For completeness, the best fit line is also included for the half fuel case but it is clearly of doubtful value.

The roll results obtained are shown in Table 4. The moment of inertia of the rig was calculated from the known geometry of the components used.

It is shown in Fig. 11 that the damping, expressed as the logarithmic decrement, of the roll oscillations of the complete aircraft is relatively high and depends heavily on fuel state, but only slightly on roll amplitude. The damping of the aircraft wings alone is shown in Fig. 12 as a function of fuel state and is seen to be only slightly less than the mean damping of the complete aircraft, also included in the figure; there was no detectable dependence of the damping of the wings alone on roll amplitude. The measured dampings are not sufficiently high for the measured periods to differ significantly from the true undamped values.

Because of the reduction in period as the amplitude decreased, (due to the damping), the measured oscillation periods were obtained from the time for only 1 cycle; their accuracy is estimated to be ± 0.003 sec in about 1·5 sec. It is estimated that the process of fitting straight lines to the data, leads to errors of less than ± 0.2 per cent in the value of P_x at zero amplitude for the empty and full cases, and to a corresponding error in the corrected inertia about the centre of gravity of about 0·8 per cent. The total inertia error, before deduction of the virtual inertia, is estimated to be about ± 2 per cent; the additional error comes mainly from the estimated error of ± 0.5 inch in the height of the aircraft centre of gravity, which affects the axis transfer term. The total error in the derived effective flight values of the aircraft inertia is estimated to be about ± 3 per cent when the estimates of virtual inertia, assumed accurate to ± 20 per cent, are included, and the flight inertias in Table 4 have been rounded off to correspond to this accuracy. It is not possible to estimate an error for the half fuel condition, but it is clearly likely to be larger, due both to the scatter of the results and to the greater uncertainty in the height of the centre of gravity.

The comparison of the measured and calculated inertias of the additional weights shown in Table 7, does not contradict these estimates. Clearly, inertia measuring errors present in the tests both with and without the weights might cancel when determining the weight inertia; the agreement in the half fuel case may be fortuitous. The check using the additional weights demonstrates, however, that there are no unexpected errors inherent in the application of equation (3).

3.3. *Moment of Inertia in Pitch.*

It proved much easier to measure the pitching inertia than the rolling inertia. No dependence of pitch oscillation period on amplitude could be detected and the oscillations were very lightly damped for all fuel states, the logarithmic decrement being about 0·004, an order of magnitude less than even the empty aircraft roll case. The reasons for these differences between roll and pitch are discussed in Section 5.

The oscillation periods for use in equation (4) were averaged over 10 cycles for a number of runs and very consistent values of 0·854, 0·880 and 0·894 sec were obtained for the empty, half full, and fully fuelled aircraft pitching periods respectively. The derivation of the effective flight test values of the moments of inertia in pitch, from the values measured about the pitch knife edges, is shown in Table 5. The rig inertia was calculated from its known geometry.

It is estimated that the measured periods are accurate to better than 0·001 sec and that the moments of inertia, before deduction of the virtual inertia are accurate to ± 1 per cent. As in the roll tests, comparison of the measured and calculated inertias of the additional weights, shown in Table 7, does not contradict this estimate of accuracy. The error in the weight inertia is equivalent to an error of less than 1 per cent in the aircraft inertia for the half and full fuel states and to slightly greater than 1 per cent for the zero fuel state.

It is difficult to estimate the accuracy of the virtual inertia, but the error is unlikely to exceed ± 20 per cent, which would cause an additional error of about 0·5 per cent in either the structural pitching inertia or the effective flight pitching inertia about the centre of gravity.

The total error in the pitching inertia is thus unlikely to exceed 1·5 per cent and the flight test inertias in Table 5 have been rounded off to correspond to this accuracy.

3.4. *Moment of Inertia in Yaw.*

The derivation of the flight test values of the yawing moment of inertia is shown in Table 6 for the three aircraft fuel states. The yaw inertia of the aircraft plus rig was calculated from equation (6) using values of the measured yaw mode period corrected for the roll/yaw ratio of the yaw mode and for interference from the other modes of the system. The form of this correction is shown in the Appendix.

The need for the correction is shown in Fig. 13 which is a carpet plot, for various spring attachment heights on the empty aircraft, of yaw mode period *versus* the tangent of the angle made with the horizontal by the line between the front and rear spring attachment points. This carpet should collapse to a single curve[5] if there was no resultant spring side force leading to interference. The total spread of period is about 5 per cent, but the individual periods are thought to be accurate to ± 0·001 sec. The yaw inertia was determined from spring conditions with the least resultant side force. The part of the correction due to the presence of a finite roll/yaw ratio was negligible for all three fuel states; that part due to interference was larger, and equivalent to about −0·4 per cent of the calculated inertia of the aircraft plus rig for each fuel state. The product of inertia, which appears in the correction term, was not measured for the half fuel state (section 3.5) and an estimate was used in this case.

The inertia of the suspension rig was calculated from its known geometry. The rig mass was small, and its centre of gravity sufficiently close to that of the aircraft alone, so that no axis transfer from the system to the aircraft centre of gravity was necessary. The total deductions were only about 7 per cent of the empty aircraft inertia (and less for the half and full fuel states) compared with about 108 per cent and 78 per cent for the roll and pitch cases.

The estimate of the virtual inertia should be more accurate than in the roll and pitch cases since ground effects should be negligible, and the main contributor to the virtual inertia is the circular fuselage which is very similar to the configurations tested in Ref. 7.

The final values of the yawing moments of inertia should be accurate to within ± 1½ per cent. The flight test inertias in Table 6 have been rounded off to correspond to this accuracy.

It is of interest to note that the damping of both the yaw and rocking modes of the system was of the same order as the damping of the rolling oscillations of the complete aircraft and of the aircraft wings.

10

3.5. *Product of Inertia.*

This quantity is the most difficult to measure. A typical time history of yaw and roll rates is shown in Fig. 14. The distortion of the roll rate trace due to interference from the rocking mode can be clearly seen, although the distortion is not as severe as that found in the tests on the Avro 707B[3]. The plot of yaw rate against roll rate peaks, Fig. 15, is typical of the results obtained in determining the roll/yaw ratio of the yaw mode. The worst case had about twice the scatter of that shown, and the best case had almost zero scatter. The line does not pass through the origin because both the roll and yaw rate zero datums are only nominal values; their precise positions are not significant in defining the required slope of the line. This slope is the yaw/roll ratio of the yaw mode.

However, having determined the roll/yaw ratios for the various spring positions, the analysis was still complicated by the resultant spring side force due to yaw, and the full equations of motion[6] had to be used. Equation (8), Section 2.4.2, may be written as

$$G = F \,.\, (\phi/\psi) + E \tag{9}$$

where

$$F = \left[A_T(\omega_2/\omega_1)^2 - g\{W_T h/q - \Sigma(\lambda_i z_i)\}^2 / W_T(\omega_3^2 - \omega_1^2)\,\omega_1^2 - A_T \right] \tag{10}$$

$$G = \left[\Delta(\lambda_i x_i z_i)/\omega_1^2 + g\Delta(\lambda_i x_i)\{W_T h/q - \Sigma(\lambda_i z_i)\}/W_T(\omega_3^2 - \omega_1^2)\,\omega_1^2 \right]. \tag{11}$$

Figs. 16 and 17 show plots of G against $F\,.\,(\phi/\psi)$ for the empty and full fuel cases respectively. The value of G when $F\,.\,(\phi/\psi) = 0$ is theoretically equal to the product of inertia. In the full fuel case, Fig. 17, both positive and negative values of the roll/yaw ratio, (ϕ/ψ), were obtained and the intercept when $(\phi/\psi) = 0$ is easily determined. Unfortunately, this was not possible in the empty case, Fig. 16, with the range of spring positions available. Although plotting G against $F\,.\,(\phi/\psi)$ collapses the results considerably, when compared with the published method[5] of plotting $\Delta(\lambda_i x_i z_i)/\omega_1^2$ against (ϕ/ψ), there appears to be a trend with mean spring height.

The expressions for F and G are rather complicated and contain such parameters as the swaying mode frequency, ω_3, which had to be calculated, and the geometric lengths h and q, Fig. 21, which were estimated from photographs and drawings since their significance was not realised at the time of the tests. It is perhaps not surprising that the points do not yield a single line, but it is not possible to give a definite reason for the trend with mean spring height. This point is discussed in Section 5.

However, the results for the three mean spring heights for which a number of points were available, do tend to lie on straight lines which converge towards a single point on the G axis. The mean value for this point is shown as the value of E in Fig. 16 and it is considered that this is the most satisfactory value of the product of inertia which can be extracted from these tests.

The resulting values of the aircraft product of inertia, after correcting for the rig product of inertia of 16 slug ft², are 336 and 218 slug ft² for the empty and full cases respectively, equivalent to inclinations of the principal axis of 0·8° and 0·5° nose down respectively.

It is very difficult to define the accuracy of the results, as they depend on the accuracy of calculating the correction term, due to the resultant spring side force, in G:

$$g\Delta(\lambda_i x_i)\{W_T h/q - \Sigma(\lambda_i z_i)\}/W_T(\omega_3^2 - \omega_1^2)\,\omega_1^2 \,.$$

This was typically about -300 slug ft², and could be in error by ± 40 slug ft². Thus a possible accuracy for the product of inertia is ± 60 slug ft². This is equivalent to $\pm 0\cdot1°$ in the inclination of the principal axis.

4. Comparison of Estimated and Measured Inertias.

4.1. Manufacturer's Estimates of the Aircraft Inertias.

Table 8 compares the values of the manufacturer's estimates of the moments of inertia of the Fairey Delta 2 with the measured values. The estimates were made for the empty aircraft only.

The estimates were 37 per cent too great in roll and 18 and 13 per cent too small in pitch and yaw respectively. At the time when these estimates were made, inertia estimating techniques were less refined than at present and it seems likely that very much better accuracy may now be expected[4,11], possibly 1 per cent in the zero fuel case.

Comparison of the estimated with the measured value of the nose-down inclination of the principal longitudinal inertia axis to the fuselage longitudinal datum axis is also made in Table 8. The estimate is seen to be 1·0° too great, but it must be remembered that there is some uncertainty in the measured product of inertia.

4.2. Estimates of the Fuel Inertia.

It is necessary for the analysis of dynamic flight tests to know the variation of aircraft inertia with fuel state. Neither the measurement nor the estimation of the inertia of moving fuel are straightforward and a comparison is valuable.

The tank geometry of the Fairey Delta 2 is shown in Fig. 7. The estimates of the fuel inertia were made relatively crudely; each tank was transformed into an equivalent rectangular tank holding the correct quantity of fuel at the correct tank centre of gravity position. This simplified greatly the calculation of the moments of inertia. The inertia of the fuel about the relevant tank axis was found, using the data of Refs. 8 and 9 to allow for fuel sloshing; the axis transfer to axes through the aircraft centre of gravity was made assuming that the mass of fuel was equivalent to a solid body with its centre of gravity at the tank centre of gravity. The axis transfer terms made up most of the estimated value, being about 93 per cent in roll, 97 per cent in pitch and 95 per cent in yaw of the total.

The estimated and measured values of the fuel inertia are compared in Table 9. Considering the simplicity of the method of estimation, it is felt that the agreement is remarkably good. The agreement between the roll inertias for half fuel may be fortuitous on account of the large scatter in the measured periods and the uncertain aircraft centre of gravity height. It is seen that in pitch, the differences between the measured and estimated fuel inertias are rather less than those between the estimated and measured values of the inertia of the additional weights, Table 7. This is apparently surprising since the weight inertia was estimated very accurately, but, expressed as a percentage of the aircraft inertia, both sets of differences are within the estimated overall measuring accuracy of 1·5 per cent, Section 3.3, and no significance can be attached to their relative sizes. However, the error in the estimated fuel inertias may be fortuitously small.

It should be remembered that the fuel inertia discussed here is strictly an effective mean value since, in general, the inertia of fuel in a moving tank varies continuously, particularly if the tank is not full.

Fig. 18 is a plot of the aircraft inertias, transferred to principal axes, *versus* fuel gone. The measured values shown were calculated from the sea level values given in Tables 4 to 6. The estimated values were obtained by adding estimated fuel inertias to the measured sea level empty aircraft inertia (2464 lb of fuel gone) and transferring to principal axes: agreement is therefore forced between measured and estimated values for the empty aircraft. The fuel inertia estimates were made for those fuel states where individual tanks became full and for the half fuel case, that is for states 3, 4, 5 and 9 in Table 2; the inertia of the fuel in the fuselage collector tank was included. The inclination of the principal axis for the intermediate fuel states was taken as 0·6°, derived from a mean of the products of inertia of the empty and full aircraft. The data points on the graphs were joined by straight lines as further accuracy was not justified.

Although the agreement between the measured and estimated inertias is within the estimated accuracy of the measurements, it should be pointed out that the fuel load of the Fairey Delta 2 is only about 20 per cent of the aircraft's empty weight. This is low compared with most aircraft and errors in fuel inertia estimation would generally be more significant.

12

5. Discussion of Results.

The need for moment of inertia measurements is demonstrated by the comparison, in Table 8, of the manufacturer's estimates with the measured values of the moments of inertia. Accurate values of the Fairey Delta 2 inertias were essential for the research flying upon which this aircraft was engaged but it is clear that the estimates were unsatisfactory.

The Fairey Delta 2 estimates were of course made some years ago, the aircraft having first flown in 1954, and it seems likely that improvements in inertia estimating techniques have made estimates more reliable[4,11]. However, until there is a sufficient body of evidence to confirm this, the need for inertia measurements continues.

One must remember, however, that the techniques of inertia measurement still leave much to be desired. Prior to the present investigation. the measurement of roll and pitch inertias by the method of spring restrained oscillations about knife edges was considered to be straightforward. The relationship between roll amplitude and period found for the Fairey Delta 2 had not been noticed before. This phenomenon could have been present and not noticed during earlier tests at R.A.E.[3,4] since the effect of varying roll amplitude was not explicitly investigated.

The reason for this effect is not known. The roll amplitudes used were too small to introduce geometric second order terms and the sinusoidal form of the roll motion suggested that no other significant non-linear terms were present. The variation of roll period with roll amplitude was much more marked for the complete aircraft than for the aircraft wings alone and was absent during the pitching oscillations. The reason for the variation must, therefore, be sought in the differences between the three experimental systems. Fuel sloshing was eliminated as the cause since the effect was present for the completely empty wings alone. The two major differences between the complete aircraft and the wings rig, apart from the geometric absence of the fuselage and fin, were that the weight of the aircraft was much greater than that of the wings and that the wings alone were rather higher above the ground than the complete aircraft wings.

There may possibly be some mechanical effect at the knife edges which leads to an increase of oscillation period with amplitude, and this effect may be accentuated by increasing the load on the knife edges, but this is unlikely, since the system weight was closely the same in the pitch tests and the knife edges used were the same. Even though the pitch inertia was very much greater, the effect, had it been present, should still have been detectable. Flexibility of the knife edge and spring supports is a possibility but measurements made at the time of the tests suggested that no significant flexibilities were present.

Alternatively, there may be some form of ground effect or 'cushioning' present during the oscillations which would be accentuated by closer proximity of the oscillating body to the ground. One might then expect some manifestation of the problem during the pitching inertia measurements, although the position of the pitching axis in relation to the overall wing area might lead to less ground effect. It is suggested that a programme of tests using a model oscillated at various heights above the ground would be useful.

When deriving the roll inertia, it seems reasonable to use the value of roll period corresponding to zero roll amplitude since one might expect that any ground effect should then tend to zero. If there is some mechanical defect at the knife edges, one might again expect the zero amplitude period to correspond most closely to the true period. The use of the zero amplitude period is supported by the steady increase of period with amplitude of the wings alone, even at the relatively large values of roll amplitude used then.

The variation, shown in Fig. 12, of the roll damping of the aircraft wings with fuel state is very significant. Mean values of the damping of the complete aircraft, from Fig. 11, are included, and are seen to be slightly higher than those of the wings alone, although showing a similar dependence on fuel state. The presence of the fuselage and fin on the complete aircraft may contribute to the increased damping in this case.

The opportunity was taken during the nominally empty and full fuel yawing moment of inertia tests to excite the rocking mode of the system and to measure its damping. This mode is mainly a rolling motion and it was found that its damping was very close to that of the roll system at the same fuel states. Its period was rather less, being about 1 sec for both fuel states. Unfortunately this test was not made at the half fuel condition but it seems likely that the relatively high level of damping on both roll rigs, and on the yaw

13

rig in roll, at zero fuel and full fuel, is related to the aircraft rather than to the suspension system. The very low damping during the pitching inertia tests at zero and full fuel may thus be related to the different positions of the oscillation axes, rather than to reduced friction in the suspension system. The damping and periods of the yaw mode of the yaw system were comparable to those of the roll system.

The variation of roll damping with fuel state may appear in a similar manner in flight. One might expect any effect to be most noticeable on the damping in roll derivative l_p and it is possible that some of the scatter in the values of l_p derived from Dutch roll tests on the Fairey Delta 2[12] could be due to this.

There was no significant variation of damping with fuel state during the pitch tests. This is probably due to the different oscillation mode and frequency failing to excite the fuel sloshing modes to the same extent, coupled with the much greater inertia of the pitching system. The lack of scatter on the measured periods for the half fuel condition during the pitching tests, compared with the large scatter during the comparable rolling tests, probably has the same cause.

The interference problems associated with the Fairey Delta 2 yaw and product of inertia rig might lead one to the conclusion that the single point suspension method is inherently unsatisfactory and that a tri-filar suspension[4], which is immune to interference problems, should be preferred. However, the tri-filar suspension method suffers from the need for a relatively massive suspension rig, and Woodfield's new analysis gives both design criteria for a single point suspension rig and a more complete analysis than Boucher et al[5].

It should be stressed that the calculation of the moment of inertia in yaw did not present any particular problems. The resultant spring side force due to the flexibility of the spring attachment brackets was undesirable, and made the extraction of the yaw inertia more complicated, but the accuracy of the result is not expected to be significantly degraded. It should not be difficult to eliminate this feature in future tests.

The failure of equation (8) to collapse the results shown in Fig. 16 on to a straight line, cannot be considered as a failure of this new method, which was developed after the tests were completed and when it was found impossible to analyse the results using Boucher's method[5]. Woodfield's analysis reveals criteria for yaw rig design to which the Fairey Delta 2 rig did not conform. In particular the flexibility of the spring supports led to most of the interference problems; the spring stiffness correction necessary due to this flexibility may itself not have been adequate. In addition the need for a number of unexpected measurements of the rig suspension geometry became apparent. It was necessary to scale the quantities required from photographs or drawings, and the resulting accuracy was limited. There was also some uncertainty in the roll inertia, A_T, of the complete system, required in equation (8).

There was no difficulty in extracting the roll/yaw ratio of the yaw mode in the presence of appreciable interference in the roll motion. The method did in fact collapse the results very considerably to yield Fig. 16, particularly for those spring attachment points closest to the centre of gravity of the system. It is not clear why the results for attachment points further below the centre of gravity showed less inclination to collapse.

A possible explanation for the poorer results from the lower points is that the spring support bracket flexibility was more significant for the longer cantilever lengths associated with the lower attachment positions. The spring and support bracket stiffnesses were measured separately and combined to obtain a total stiffness. This procedure may have introduced errors which would be likely to be more significant for the longer bracket lengths and it is recommended that the stiffness of the restraining springs for all inertia measuring rigs should be calibrated in situ.

It is useful to illustrate the extent to which the Fairey Delta 2 rig failed to conform to the design criteria developed by Woodfield. The product of two parameters in particular, $\Delta(\lambda_i x_i)$ and $\{W_T h/q - \Sigma(\lambda_i z_i)\}$, should be zero or as small as possible. For the Fairey Delta 2 rig a typical value of the former was 2000 lb, and of the latter was 10 000 lb and it is instructive to compare these values with those of 0 and -65 lb considered by Woodfield for the design case he illustrates[6]. The Fairey Delta 2 rig is then seen to have been very badly designed, albeit unwittingly.

It is clear that a yaw inertia rig should be designed to Woodfield's principles so that a true evaluation of his method can be made. Such an opportunity will occur shortly during further tests planned at R.A.E. Bedford. Measurements will be made to determine the yaw and product of inertia both of an aircraft,

and of some simple body, such as a homogeneous circular cylinder at incidence, the inertia of which can be accurately calculated.

6. *Conclusions and Recommendations for Further Work.*

The moments and product of inertia of the Fairey Delta 2 aircraft have been measured using the method of spring restrained oscillations. The moment of inertia results were satisfactory, but difficulty was found in determining the product of inertia due to unsatisfactory design of the single point suspension rig.

A dependence of roll period on roll amplitude was discovered and this may be due to some form of ground effect. The damping in roll was found to vary with fuel state.

The agreement between the manufacturer's estimates and the measured moments and product of inertia was poor, and there is clearly a continuing need for inertia measurements. Simple estimates of the fuel inertias compared well with the measured values, agreement being within the expected accuracy of the measurements. The Fairey Delta 2 fuel load is, however, relatively small, and simple estimates for greater loads might be less satisfactory.

It is recommended that yawing inertia tests should be made both on an aircraft, and on a simple geometric body, using a correctly designed single point suspension rig, in order to confirm the adequacy of the new analysis method used in this Report for such a rig.

Model tests are needed to investigate the virtual inertia associated with delta or highly swept wings, and also to investigate the possible effect of ground proximity on the relationship between oscillation period and amplitude.

LIST OF SYMBOLS

Symbol	Unit	Definition
a	ft	Height of crane hook above spreader frame
$A_{K.E.}$	slug ft^2	Total roll inertia about roll knife edges
A_T	slug ft^2	Total roll inertia about yaw system centre of gravity
b	ft	Mean distance of yaw system centre of gravity below suspension attachment points
$B_{K.E.}$	slug ft^2	Total pitch inertia about pitch knife edges
C_T	slug ft^2	Total yaw inertia about yaw system centre of gravity
d_1	ft	Distance of mainwheel reaction behind cg datum
d_2	ft	Distance between nosewheel and mainwheel reactions
E	slug ft^2	Product of inertia
F	slug ft^2	Composite variable, see equation (10)
g	ft/sec^2	Acceleration due to gravity
G	slug ft^2	Composite variable, see equation (11)
h	ft	$a+b$
h_1	ft	Height of crane jib above hook
h_2	ft	Mean height of spreader frame above suspension attachment points
l_p	rad^{-1}	Damping in roll derivative
L	lb ft	Rolling moment
M	lb ft	Pitching moment
N	lb ft	Yawing moment
P	sec	$2\pi/\omega_3$, period of swaying mode
P_x	sec	Roll period
P_y	sec	Pitch period
P_z	sec	$2\pi/\omega_1$, period of yawing mode
q	ft	h_1+h_2
R_M	lb	Total mainwheel reaction
R_N	lb	Nosewheel reaction
T, T_i	lb	General spring tension
T_L	lb	Port roll spring tension
T_0	lb	Spring tension in equilibrium position
T_R	lb	Starboard roll spring tension
W_T	lb	Weight of aircraft plus inertia rig
x_F	ft	Distance of front springs ahead of yaw suspension axis

16

Symbol	Unit	Definition
x_i	ft	General yaw spring distance ahead of yaw suspension axis
x_R	ft	Distance of rear springs aft of yaw suspension axis
x_s	ft	Distance of springs ahead of pitch knife edges
$\bar{x}$	ft	Distance of aircraft centre of gravity aft of cg datum
$\bar{x}_T$	ft	Distance of pitch system centre of gravity ahead of pitch knife edges
y_s	ft	Distance of springs outboard of roll knife edges
z_i	ft	General yaw spring height below yaw system centre of gravity
$\bar{z}$	ft	Height of aircraft centre of gravity above cg datum
$\bar{z}_T$	ft	Height of roll and pitch systems centre of gravity above knife edges
θ	deg	Angular displacement in pitch
λ_F	lb/ft	Combined effective stiffness of front yaw springs
λ_i	lb/ft	General effective yaw spring pair stiffness
λ_R	lb/ft	Combined effective stiffness of rear yaw springs
λ_x	lb/ft	Combined stiffness of roll springs
λ_y	lb/ft	Combined stiffness of pitch springs
ϕ	deg	Angular displacement in roll
ψ	deg	Angular displacement in yaw
ω_1	rad/sec	Natural frequency of yawing mode
ω_2	rad/sec	Natural frequency of rocking mode
ω_3	rad/sec	Natural frequency of swaying mode

17

REFERENCES

No.	Author(s)	Title, etc.

1   N. J. DeLeys .. .. ..   A review of various techniques for measuring the moments and products of inertia of aircraft.
Cornell Aeronautical Laboratory FDM 342 (1963).

2   J. Clark.. .. .. ..   Measurement of the moment of inertia of a Hunter 2 aircraft.
R.A.E. Technical Note Aero 2615 (1959).

3   D. H. Perry .. .. ..   Measurements of the moments of inertia of the Avro 707B aircraft.
A.R.C. C.P. 647 (1961).

4   L. J. Fennell .. .. ..   Measurements of the moments of inertia of the Handley Page HP 115 aircraft.
A.R.C. C.P. 907 (1965).

5   R. W. Boucher, D. A. Rich ..   A method for measuring the product of inertia and the inclination
H. L. Crane and C. E. Matheny   of the principal longitudinal axis of inertia of an airplane.
NACA Technical Note 3084 (1954).

6   A. A. Woodfield .. ..   Measurement of the yawing moment and product of inertia of an aircraft by the single point suspension method: theory and rig design.
A.R.C. R. & M. 3607 (1968).

7   F. S. Malvestuto and .. ..   Formulas for additional mass corrections to the moments of
L. J. Gale   inertia of airplanes.
NACA Technical Note 1187 (1947).

8   E. Widmayer and J. R. Reese..   Moment of inertia and damping of fluid in tanks undergoing pitching oscillations.
NACA RM L53E01a, (TIB 3763) (1953).

9   J. R. Reese and J. L. Sewall ..   Effective moment of inertia of fluid in offset, inclined, and swept-wing tanks undergoing pitching oscillations.
NACA Technical Note 3353 (1955).

10   J. S. Thompson, R. A. Fail ..   Low speed wind tunnel measurements of the oscillatory lateral
and J. V. Inglesby   stability derivatives for a model of a slender aircraft (HP 115) including the effects of frequency parameter.
RAE Technical Report 69018 (1969) A.R.C.31289.

11   D. Hope .. .. ..   Buccaneer S, Mk. 1. Measurement of the moment of inertia of the fourth development aircraft (XK 489) Hawker Siddeley Aviation Ltd., Hawker Blackburn Division Report No. YMT 2623 (1964).

12   R. Rose.. .. .. ..   Flight measurements of the Dutch roll characteristics of a 60 degree delta wing aircraft (Fairey Delta 2) at Mach numbers from 0·4 to 1·5 with stability derivatives extracted by vector analysis.
A.R.C. C.P. 653 (1963).

APPENDIX

Equations of Motion in Roll, Pitch and Yaw.

A.1. Equation of Motion in Roll.

Referring to Fig. 19, since the spring attachment point in the equilibrium position is at the same height as the knife edges, there is negligible lateral displacement of the springs for small oscillations and hence negligible lateral spring force components.

Taking moments about the knife edges in the displaced state:

$$L = W_T \bar{z}_T \sin \phi - (T_0 + \Delta T_L) y_s \cos \phi + (T_0 - \Delta T_R) y_s \cos \phi .$$

To the first order of small quantities:

$$L = W_T \bar{z}_T \phi - (\Delta T_L + \Delta T_R) y_s$$

and

$$\Delta T_L + \Delta T_R = \lambda_x y_s \phi$$

where λ_x is the total spring rate.

For motion about the knife edges:

$$A_{\text{K.E.}} \ddot{\phi} = L$$

therefore

$$A_{\text{K.E.}} \ddot{\phi} = W_T \bar{z}_T \phi - \lambda_x y_s^2 \phi .$$

Hence

$$A_{\text{K.E.}} = (P_x/2\pi)^2 (\lambda_x y_s^2 - W_T \bar{z}_T) \tag{3}$$

where P_x is the period of the roll motion.

A.2. Equation of Motion in Pitch.

Referring to Fig. 20, since the spring attachment point in the equilibrium position is at the same height as the knife edges, there is negligible fore and aft displacement of the springs for small oscillations and hence negligible longitudinal spring-force components.

In the equilibrium position:

$$T_0 x_s - W_T \bar{x}_T = 0 . \tag{A.1}$$

Taking moments about the knife edges in the displaced state:

$$M = (T_0 - \Delta T) x_s \cos \theta - W_T (\bar{x}_T \cos \theta - \bar{z}_T \sin \theta) .$$

To the first order of small quantities:

$$M = (T_0 - \Delta T) x_s - W_T (\bar{x}_T - \bar{z}_T \theta) \tag{A.2}$$

19

and
$$\Delta T = \lambda_y x_s \theta \tag{A.3}$$

where λ_y is the total spring rate.

Substituting into equation (A.2) for T_0 and ΔT from equations (A.1) and (A.3) gives:

$$M = -\lambda_y x_s^2 \theta + W_T \bar{z}_T \theta .$$

For motion about the knife edges:

$$B_{\text{K.E.}} \ddot{\theta} = M$$

therefore

$$B_{\text{K.E.}} \ddot{\theta} = -\lambda_y x_s^2 \theta + W_T \bar{z}_T \theta$$

Hence

$$B_{\text{K.E.}} = (P_y/2\pi)^2 (\lambda_y x_s^2 - W_T \bar{z}_T) \tag{4}$$

where P_y is the period of the pitching motion.

A.3. Equation of Motion in Yaw.

To use the analysis method of Boucher et al[5], the period of the system yaw mode is required when the roll/yaw ratio of the mode is zero. This period would normally be derived by plotting measured periods versus roll/yaw ratio for a variety of spring heights, and hence reading off the period corresponding to zero roll/yaw ratio, but the variation of period with roll/yaw ratio should be very small. Unfortunately, during the tests on the Fairey Delta 2, the spring restoring moment for unit yaw varied with spring height due to the support bracket cantilever stiffness, and there was no longer a simple variation of period with roll/yaw ratio. There was also of course, the added complication of the interference from the system swaying and rocking modes, due to the variation of spring stiffness with height causing a resultant spring side force.

Accordingly the equation of motion of the aircraft is derived below for the zero roll/yaw ratio and zero interference case and a correction is given for the residual roll motion and for the interference. Runs having low roll/yaw ratio were in any case selected for the derivation of the inertia in yaw.

Since the spring attachment points and the suspension axis all lie in the plane of symmetry of the aircraft, Fig. 21, there is negligible fore and aft displacement of the springs for small oscillations. The centre of gravity of the system lies on the suspension axis.

Referring to Fig. 21, taking moments about the suspension axis gives:

$$N = \sum_{i=1}^{4} \{(T_i + \Delta T_i) x_i\} .$$

The terms $T_i x_i$ are symmetrical and cancel. The incremental moment terms are given by:

$$\sum_{i=1}^{4} \{\Delta(T_i x_i)\} = \sum_{i=1}^{4} (\lambda_i x_i^2) \psi$$

with due regard to sign, where λ_i is the spring rate. For the front spring pair put $x_1 = x_2 = x_F$ and the

20

effective combined spring rate as λ_F, and similarly for the rear spring pair with suffix R. Then:

$$N = -(\lambda_F x_F^2 + \lambda_R x_R^2)\,\psi\,.$$

For pure yawing motion about the suspension axis with no roll motion

$$N = C_T\,\ddot{\psi}$$

where C_T is the combined aircraft and rig moment of inertia.

Therefore

$$C_T\,\ddot{\psi} = -(\lambda_F x_F^2 + \lambda_R x_R^2)\,\psi\,.$$

Hence

$$C_T \quad = (P_z/2\pi)^2\,(\lambda_F x_F^2 + \lambda_R x_R^2) \tag{6}$$

where P_z is the period of the yawing motion.

A correction may be derived, using the complete analysis of Ref. 6, for the presence of coupled roll motion in the system yaw mode, and for interference from the other system modes. In order to apply this correction, the right hand side of equation (6) should be multiplied by the following factor:

$$1 + \{C^2/\Phi\Sigma(\lambda_i x_i^2) + \Delta^2(\lambda_i x_i)/Y\Sigma(\lambda_i x_i^2) - 2BC\Delta(\lambda_i x_i)/Y\Phi\Sigma(\lambda_i x_i^2)\}/(1 - B^2/\Phi Y)$$

where $B = \{W_T h/q - \Sigma(\lambda_i z_i)\}$

$\quad C = E_T\,\omega_1^2 - \Delta(\lambda_i x_i z_i)$

$\quad \Phi = A_T\,(\omega_2^2 - \omega_1^2)$

$\quad Y = W_T\,(\omega_3^2 - \omega_1^2)/g$

$\quad E_T = $ the product of inertia of the oscillating system.

In this expression the first term in the curly brackets may be regarded as the correction for the residual roll motion and the second and third terms as the correction for the interference.

TABLE 1

Fairey Delta 2—Leading Particulars.

Fuselage length	51·7 ft
Wing span	26·84 ft
Nominal centre-line chord	25·0 ft
Tip chord	1·83 ft
Gross wing area	360 ft²
Leading edge sweepback	59·9°
Trailing edge sweepback	0°
Wing incidence with respect to fuselage datum	+1·5°

Centre of gravity datum is 240 in ahead of the wing trailing edge and 14·4 in below the fuselage centreline.

TABLE 2

Fuel States for Wings Ground Rig.

Fuel state No	Fuel weight, lb, in tank number:								Total fuel lb
	1 Stbd	1 Port	2 Stbd	2 Port	3 Stbd	3 Port	4 Stbd	4 Port	
1	0	0	0	0	0	0	0	0	0
2	0	0	0	0	0	0	55	55	110
3	0	0	51	51	127	123	149	149	650
4	0	0	86	86	127	123	227	227	876
5	0	0	113	113	127	123	273	273	1022
6	55	55	113	113	127	123	383	383	1352
7	94	94	113	113	127	123	461	461	1586
8	133	133	113	113	127	123	540	540	1822
9	182	160	113	113	127	123	604	590	2012

N.B.   Underlined quantities indicate full tank.

TABLE 3

Aircraft Centre of Gravity Position.

Aircraft fuel state	Weight lb	cg Position, undercarriage down		cg Position, undercarriage up	
		Aft of datum inch	Above datum inch	Aft of datum inch	Above datum, inch
Empty	11645	104·9	12·7	103·4	15·2
Half	12889	104·2	12·6	102·8	14·9
Full	14109	105·1	13·1	103·8	15·1

TABLE 4

Moment of Inertia in Roll.

Fuel state	Aircraft weight	Moment of inertia of aircraft plus rig about the knife edges	Moment of inertia of rig about knife edges	Virtual inertia about knife edges	Axis transfer to cg	Total deduct-ions	Aircraft structural inertia about cg	Virtual inertia about cg slug ft²		Effective aircraft flight inertia slug ft²	
	lb	slug ft²	slug ft²	slug ft²	slug ft²	slug ft²	slug ft²	Sea level	40 000 ft	Sea level	40 000 ft
Empty	11 645	7419	58	202	3588	3848	3571	193	47	3800	3600
Half	12 889	8819	58	202	3897	4157	4662	193	47	4900	4700
Full	14 109	10 308	58	202	4320	4580	5728	193	47	5900	5800

24

TABLE 5

Moment of Inertia in Pitch.

Fuel state	Aircraft weight	Moment of inertia of aircraft plus rig about the knife edges	Moment of inertia of rig about knife edges	Virtual inertia about knife edges	Axis transfer to cg	Total deduct-ions	Aircraft structural inertia about cg	Virtual inertia about cg slug ft²		Effective aircraft flight inertia slug ft²	
	lb	slug ft²	slug ft²	slug ft²	slug ft²	slug ft²	slug ft²	Sea level	40 000 ft	Sea level	40 000 ft
Empty	11 645	43 872	4984	678	13 590	19 252	24 620	216	53	24 800	24 700
Half	12 889	46 633	4984	678	15 422	21 084	25 549	216	53	25 800	25 600
Full	14 109	48 089	4984	678	16 251	21 913	26 176	216	53	26 400	26 200

TABLE 6

Moment of Inertia in Yaw.

Fuel state	Aircraft weight	Moment of inertia of aircraft plus rig	Moment of inertia of rig	Virtual inertia	Total deduct-ions	Aircraft structural inertia about cg	Virtual inertia about cg slug ft²		Effective aircraft flight inertia slug ft²	
	lb	slug ft²	slug ft²	slug ft²	slug ft²	slug ft²	Sea level	40 000 ft	Sea level	40 000 ft
Empty	11 645	29 469	1795	201	1996	27 473	201	49	27 700	27 500
Half	12 889	31 274	1795	201	1996	29 278	201	49	29 500	29 300
Full	14 109	33 115	1795	201	1996	31 119	201	49	31 300	31 200

TABLE 7

*Comparison of the Calculated and Measured
Inertia of the Additional Weights.*

Aircraft fuel state	Measured weight inertia slug ft^2	
	Roll	Pitch
Empty	3102	2025
Half	3235	2128
Full	3174	2184

Calculated inertia: Roll   3219 slug ft^2
Pitch   2318 slug ft^2

TABLE 8

*Comparison of the Manufacturer's Estimates and the
Measured Values of the Aircraft Inertias.*

Axis	Fuel state	Manufacturer's estimate slug ft^2	Measured inertia slug ft^2
Roll	Empty	4900	3600
Pitch	Empty	20100	24600
Yaw	Empty	24600	27600
Inclination of principal axis	Empty	1·8°	0·8°

TABLE 9

Comparison of Estimated and Measured Fuel Inertia.

Axis	Fuel state	Estimated fuel inertia slug ft²	Measured fuel inertia slug ft²
Roll	Half Full	1058 2338	1091 2157
Pitch	Half Full	872 1602	929 1556
Yaw	Half Full	1943 3970	1805 3646

O 1 2 3 4 5 10'

SCALE - ft

FIG. 1. General arrangement of the Fairey Delta 2.
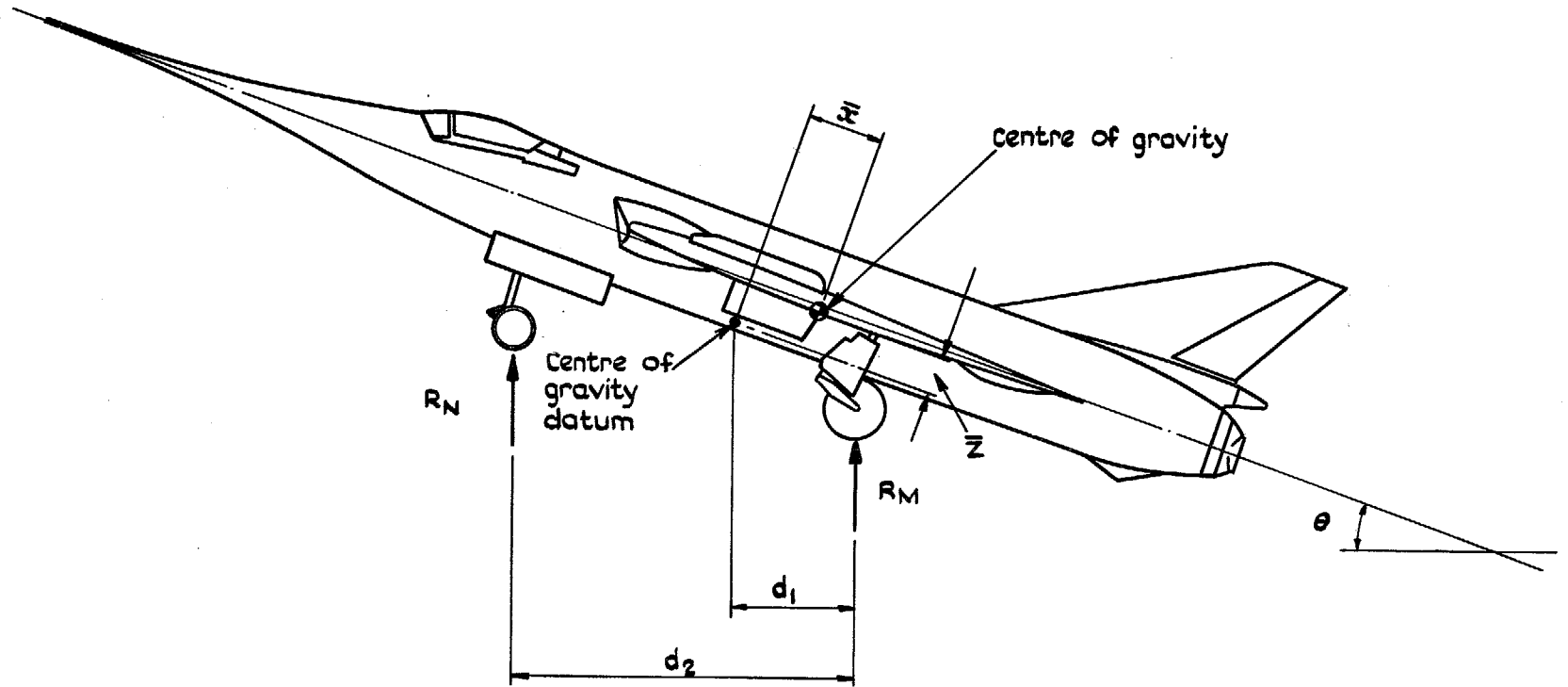
$$(R_N + R_M)(\bar{x} \cos \theta + \bar{z} \sin \theta) + R_N(d_2 - d_1) - R_M d_1 = 0$$

FIG. 2.   Determination of aircraft centre of gravity position.

FIG. 3a. Aircraft on rolling moment of inertia rig.

Aircraft cg

Base frame

Cradles   (Knife edge underboth)

Tension springs

Knife edge
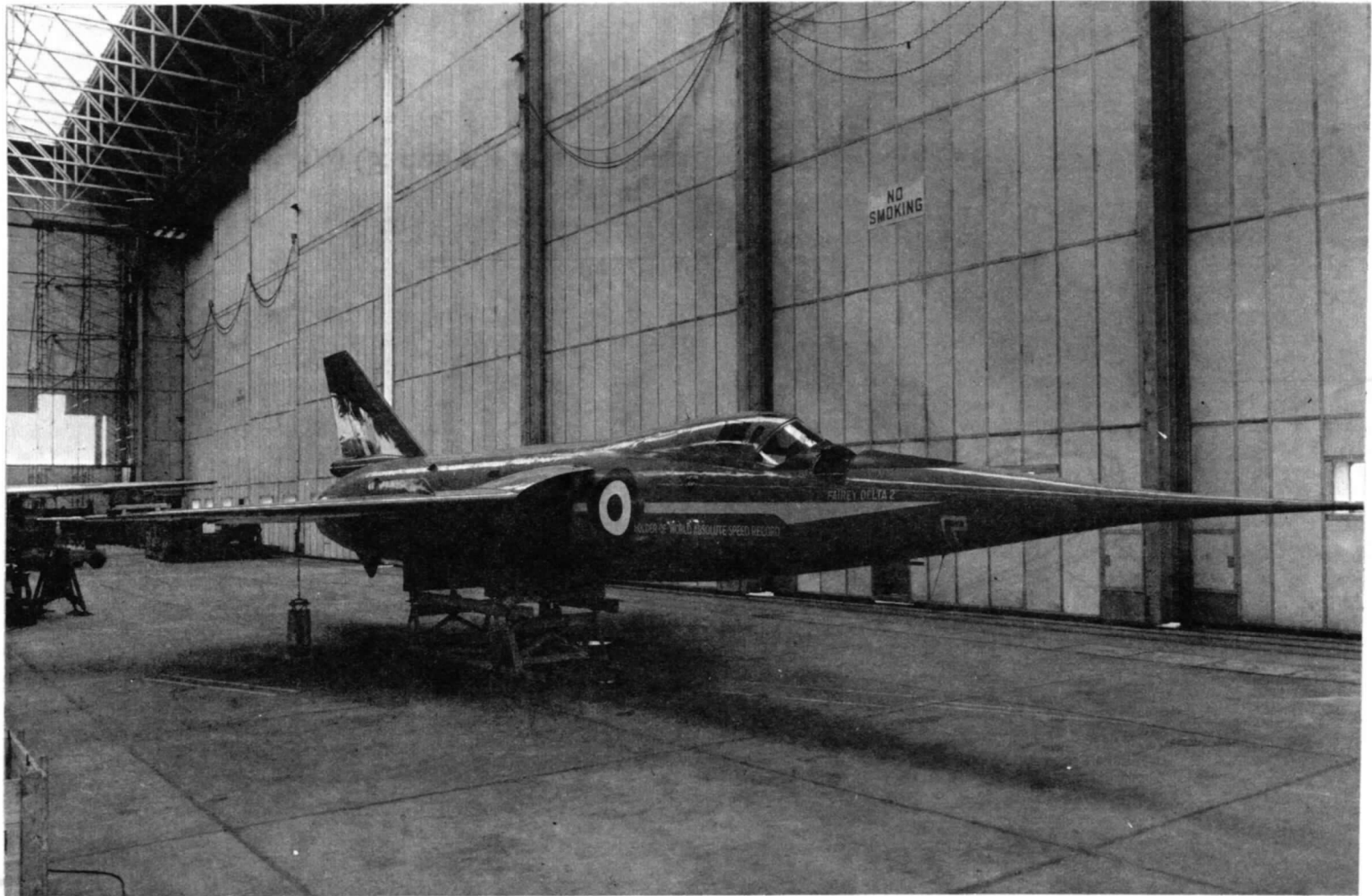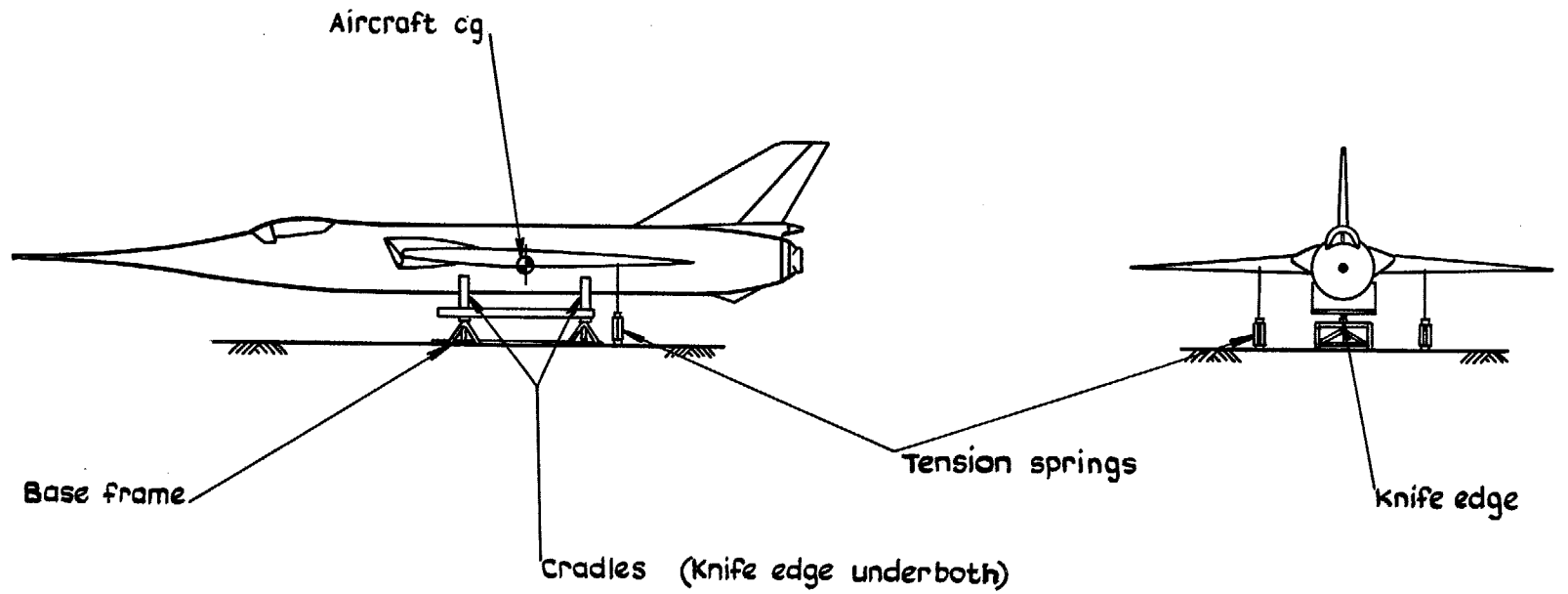
FIG. 3b.   GA of aircraft on rolling moment of inertia rig.

FIG. 4a.   Wings roll rig.

Tension springs

Base frame

Knife edge
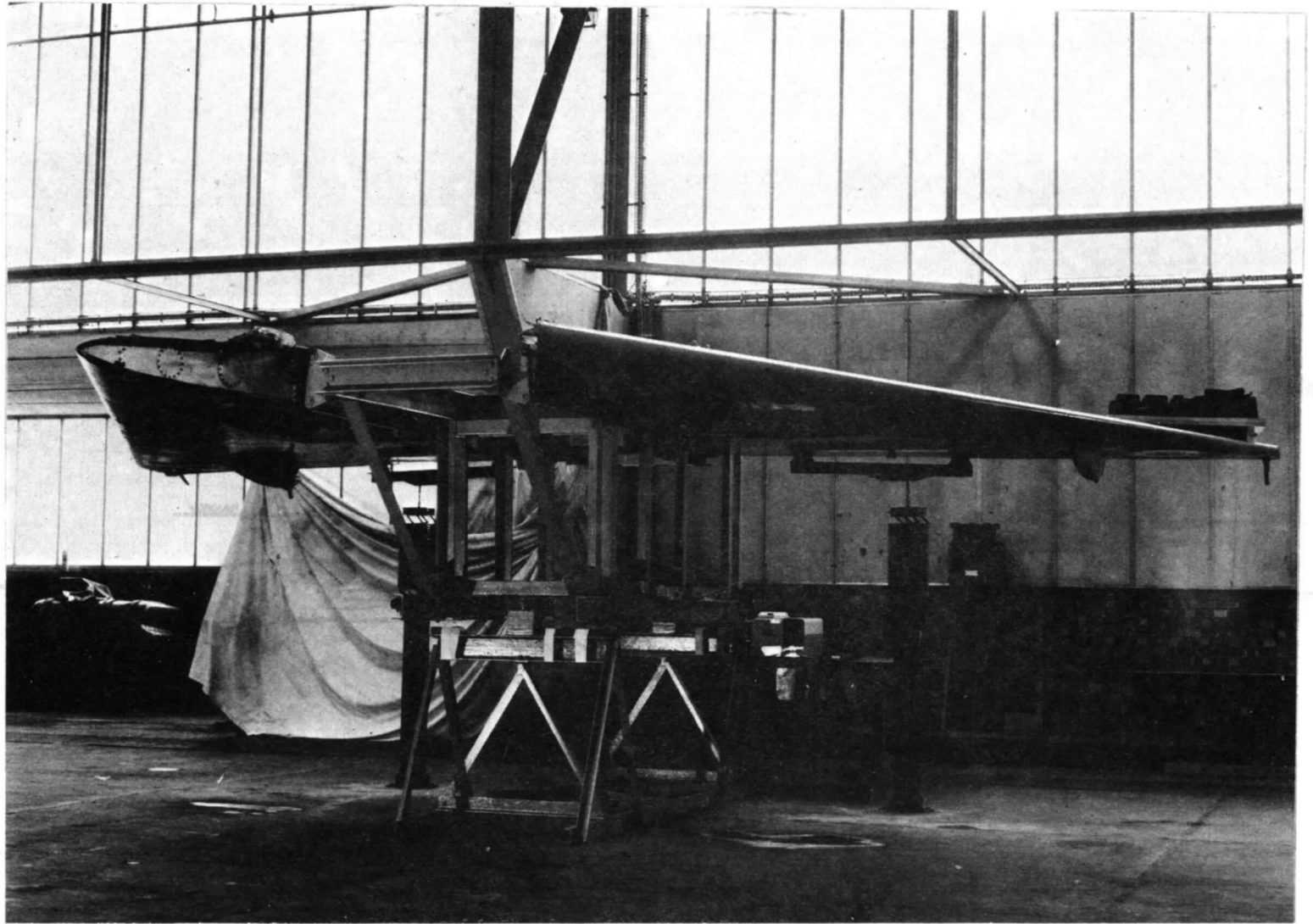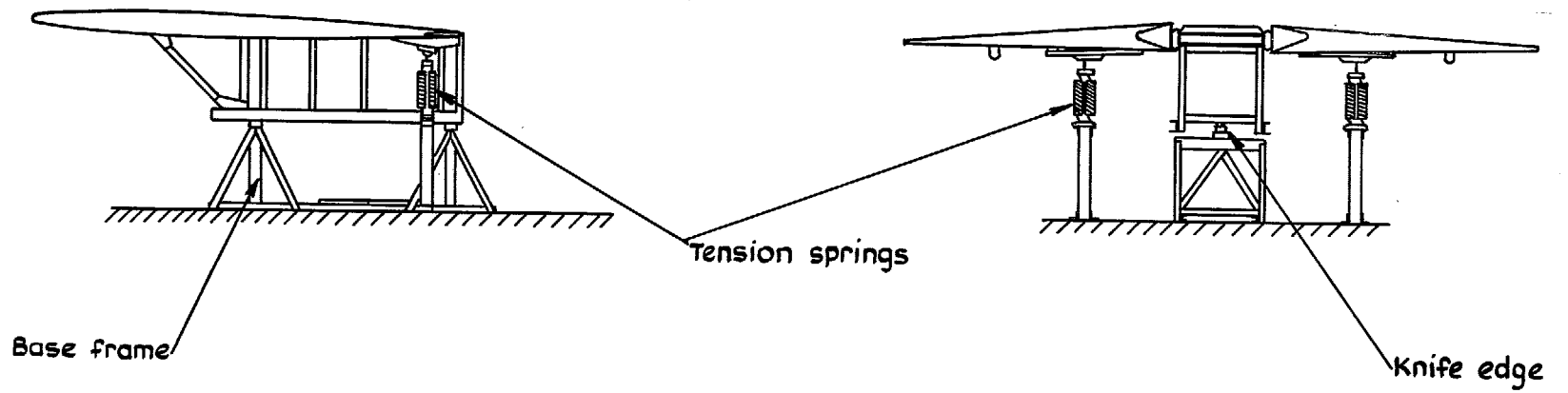
FIG. 4b.   GA of wings roll rig.

Fig. 5a. Aircraft on pitching moment of inertia rig.

Aircraft cg

Aircraft jacking bar

Tension springs

Knife edge

Nose cradle
(Forward jacks omitted
for clarity)
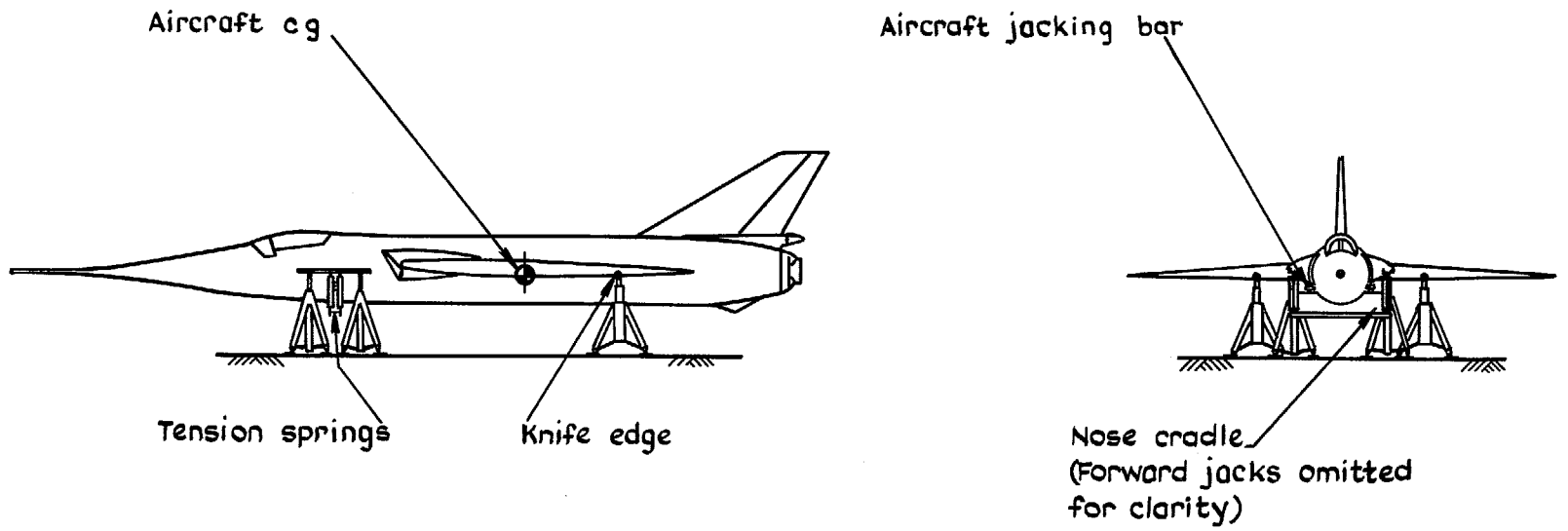
FIG. 5b. GA of aircraft on pitching moment of inertia rig.

FIG. 6a. Aircraft on yawing moment of inertia rig.

Spreader frame

Aircraft cg

Alternative spring attachment brackets

Restraining springs
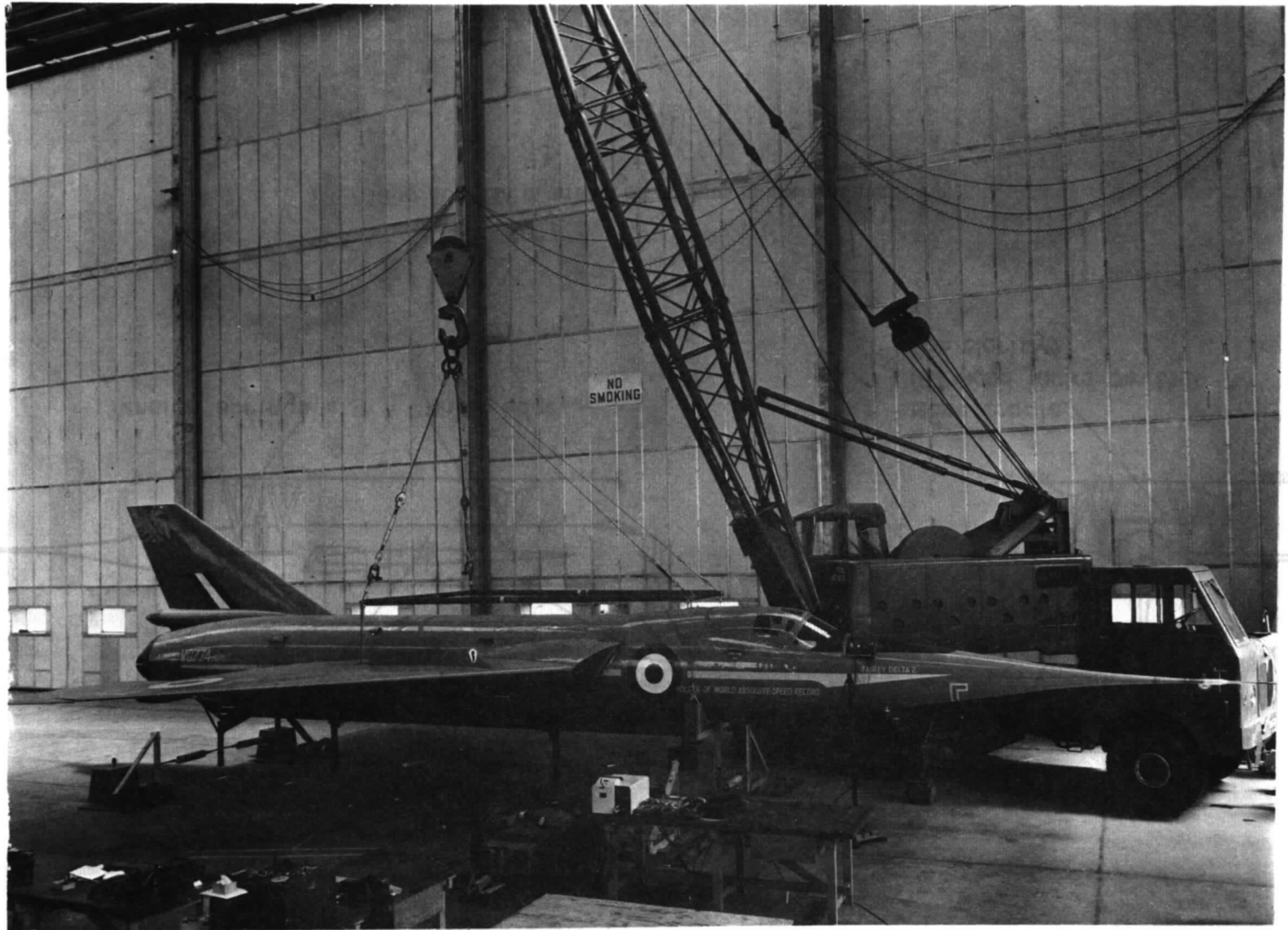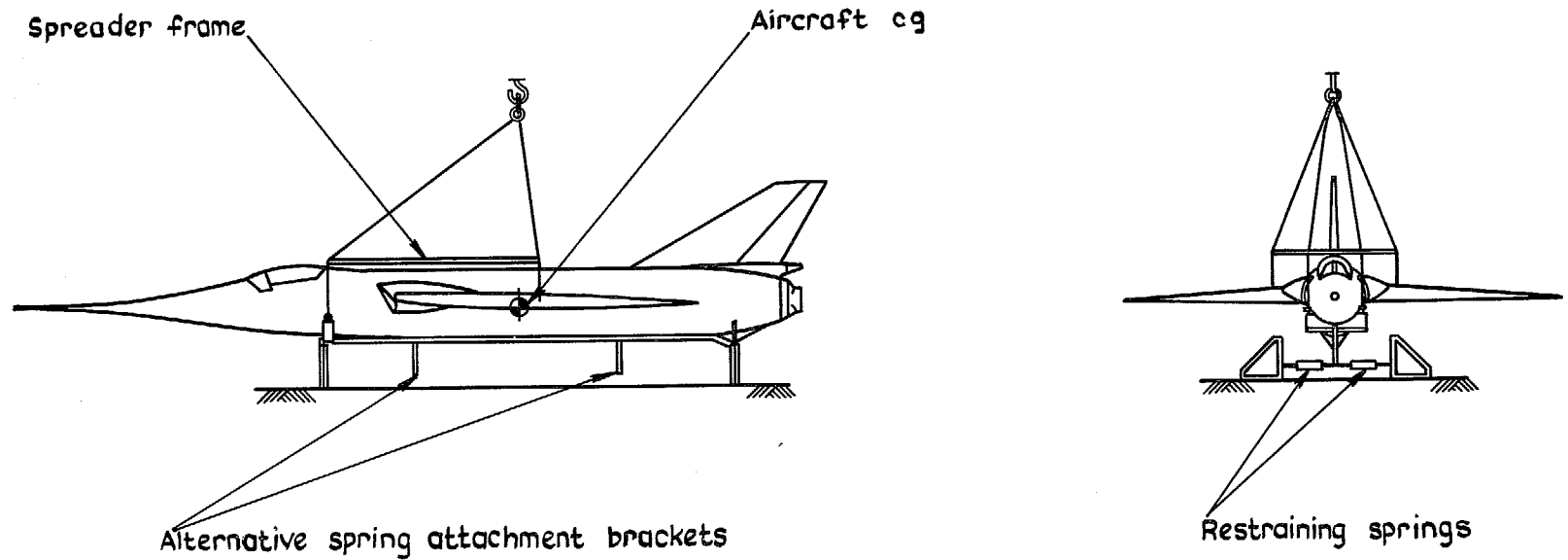
FIG. 6b. GA of aircraft on yawing moment of inertia rig.
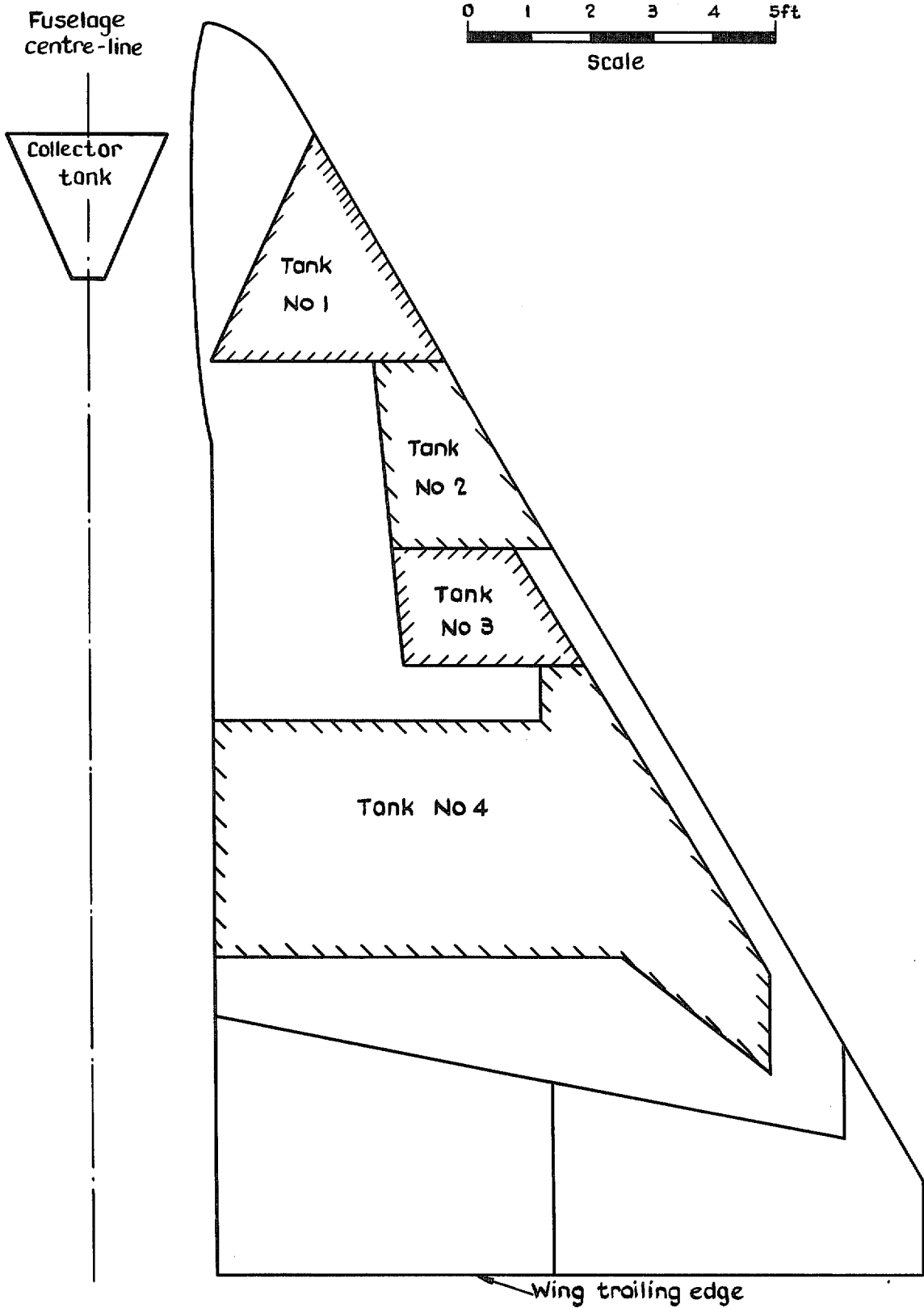
FIG. 7.   Fairey Delta 2 fuel tank layout.
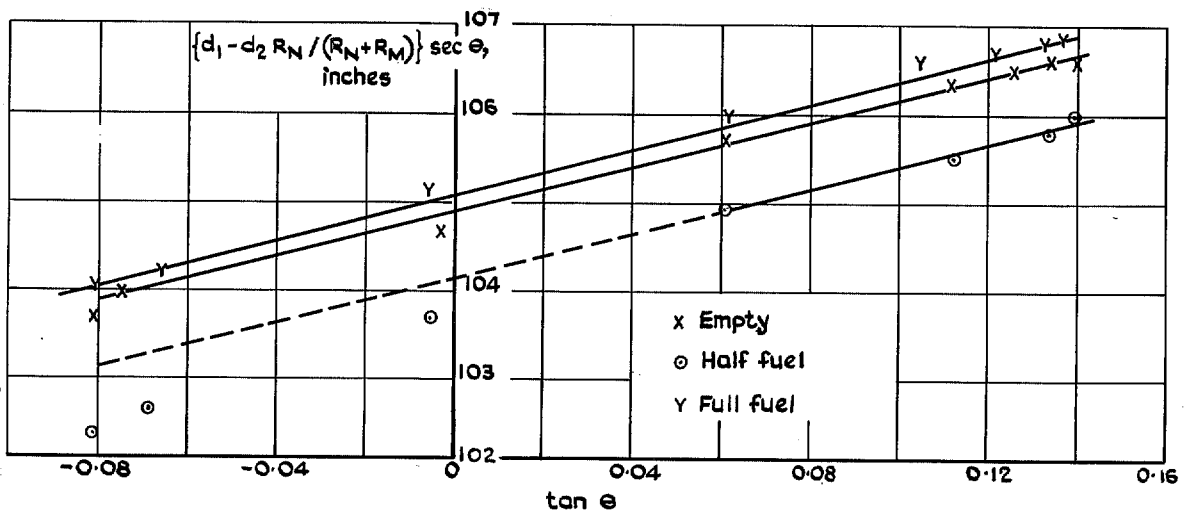
FIG. 8. Determination of aircraft centre of gravity position, undercarriage down.
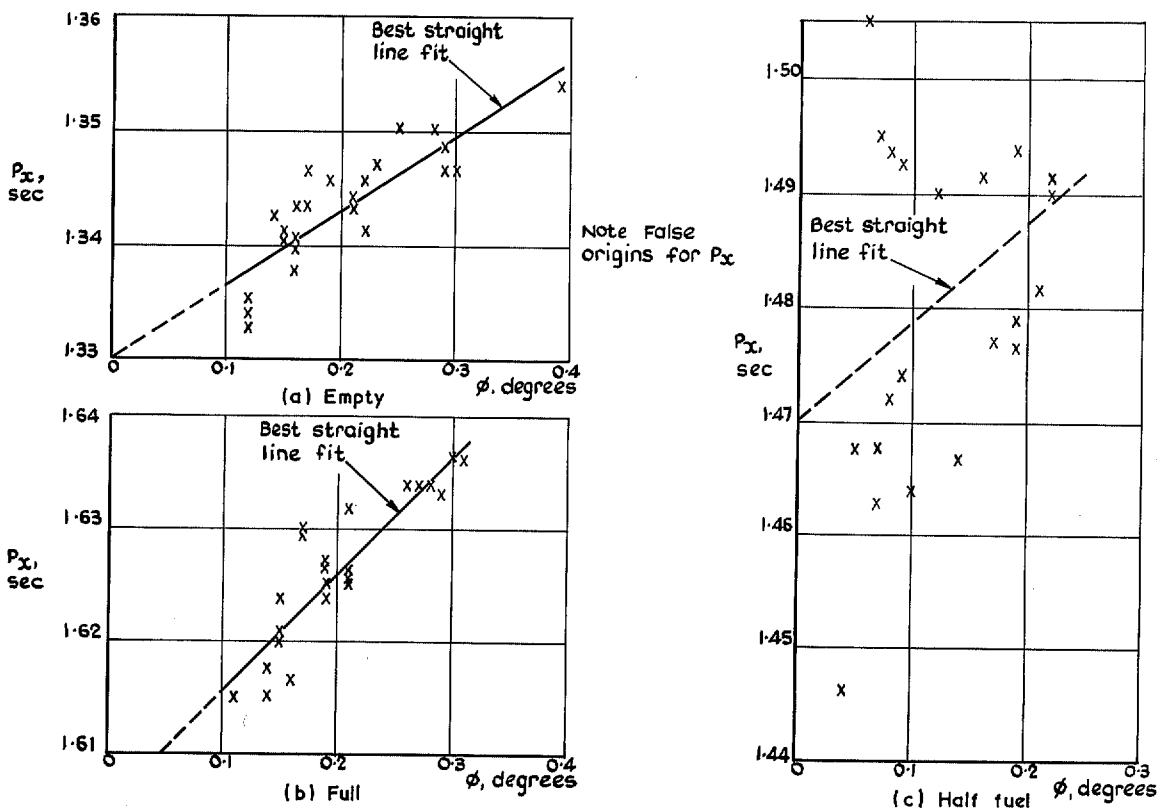
FIG. 9. Variation of roll period with roll amplitude, complete aircraft.

39
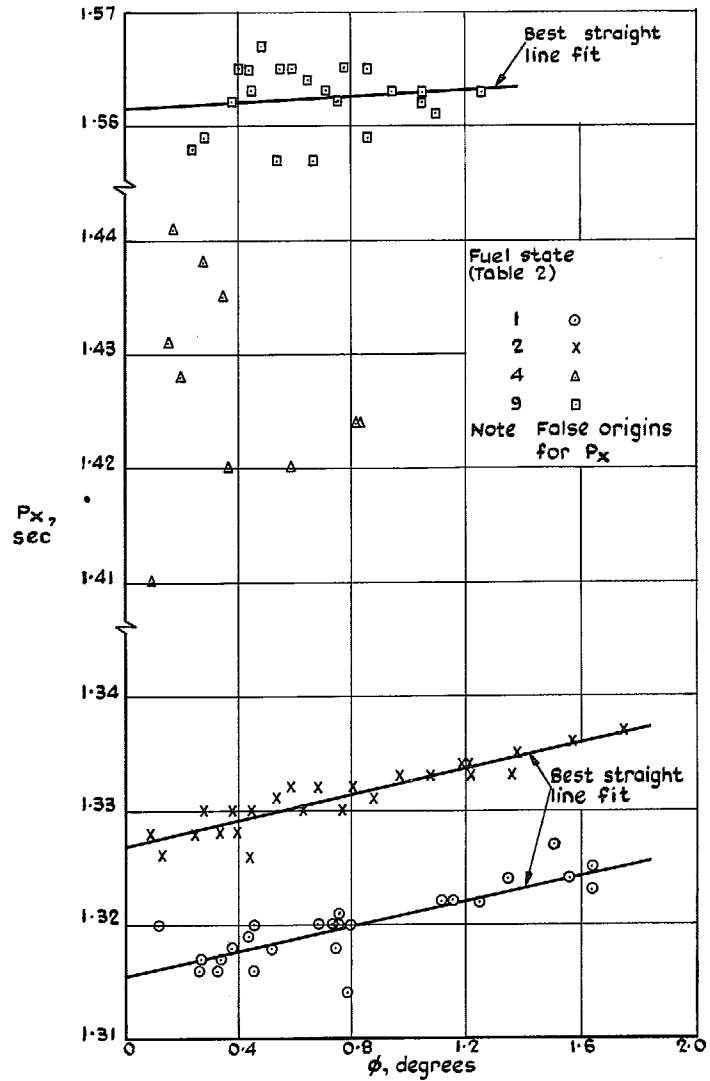
Fig. 10. Variation of roll period with fuel state
and roll amplitude on wings ground rig.
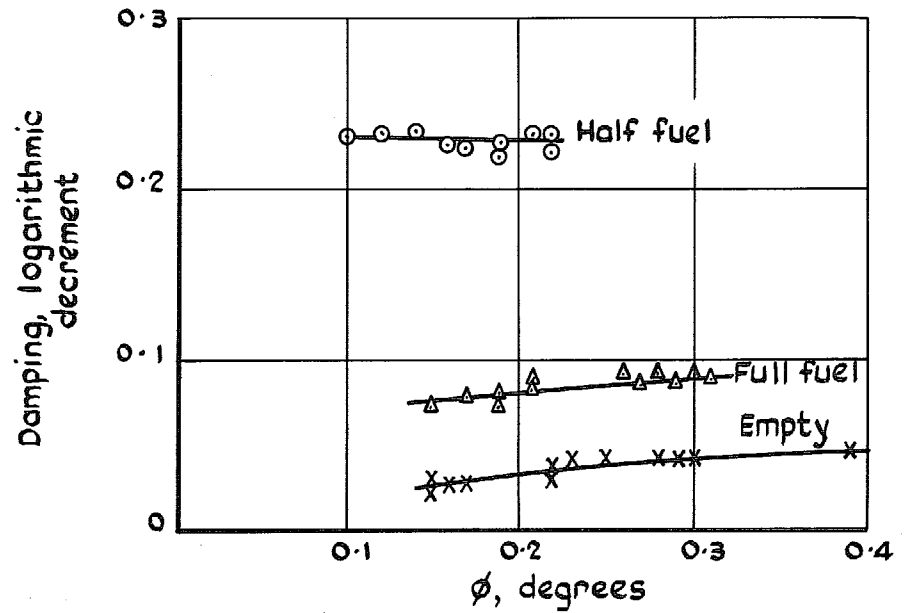
Fig. 11. Variation of roll damping with fuel state
and roll amplitude, complete aircraft.
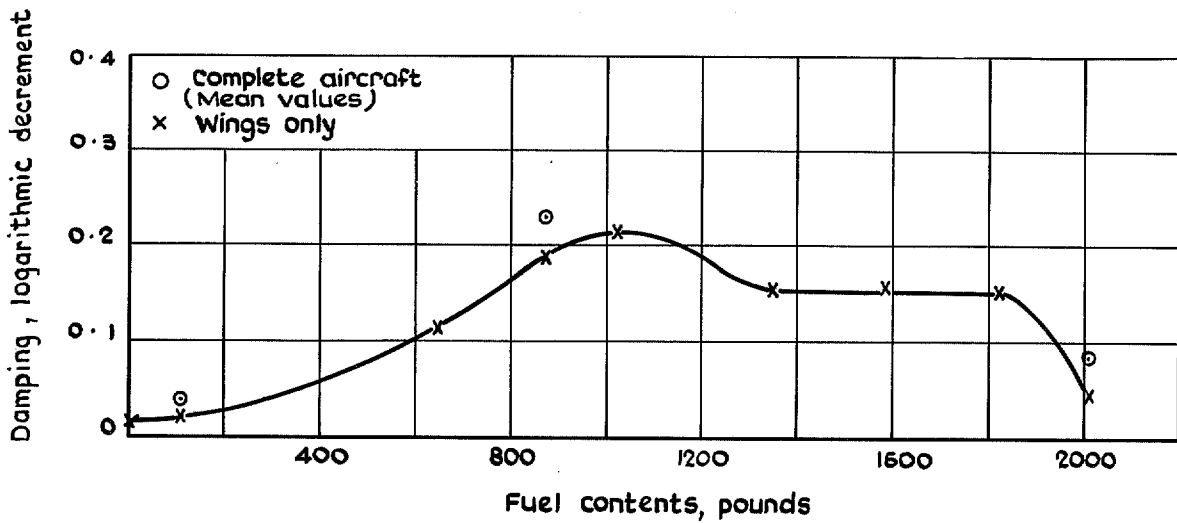
FIG. 12. Variation of roll damping with fuel contents in wings.
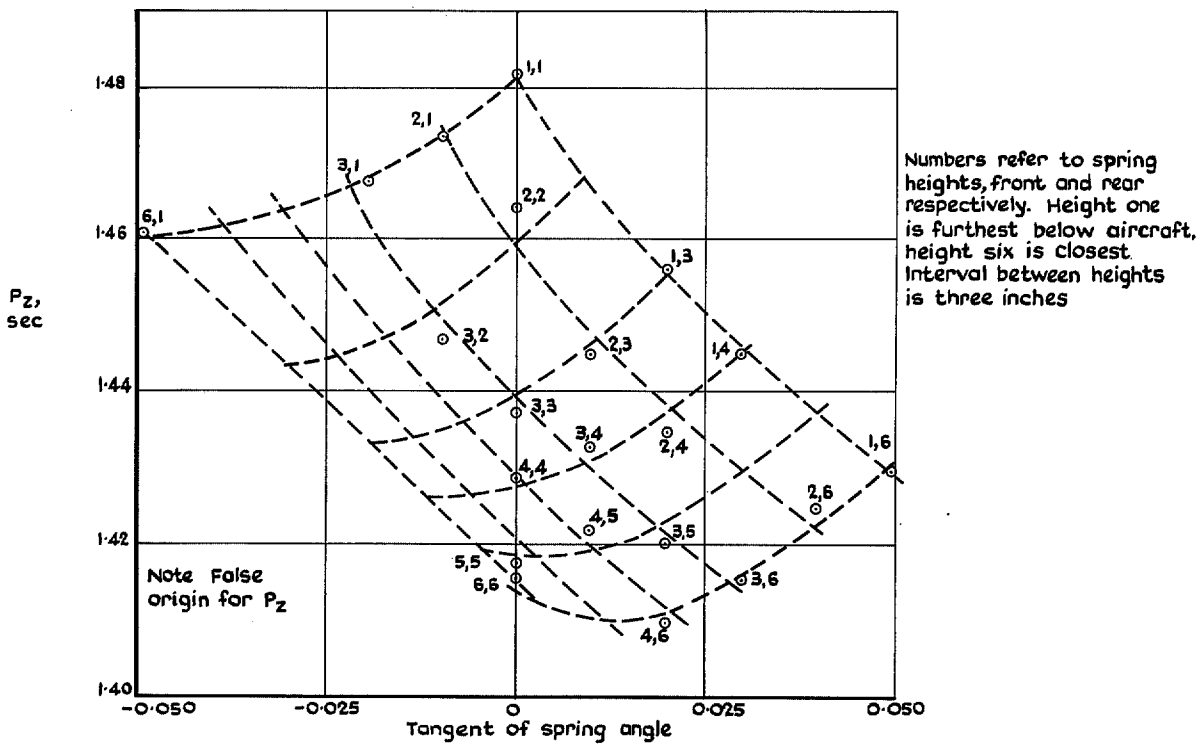
FIG. 13. Variation of yaw mode period with spring position on the empty aircraft.

41
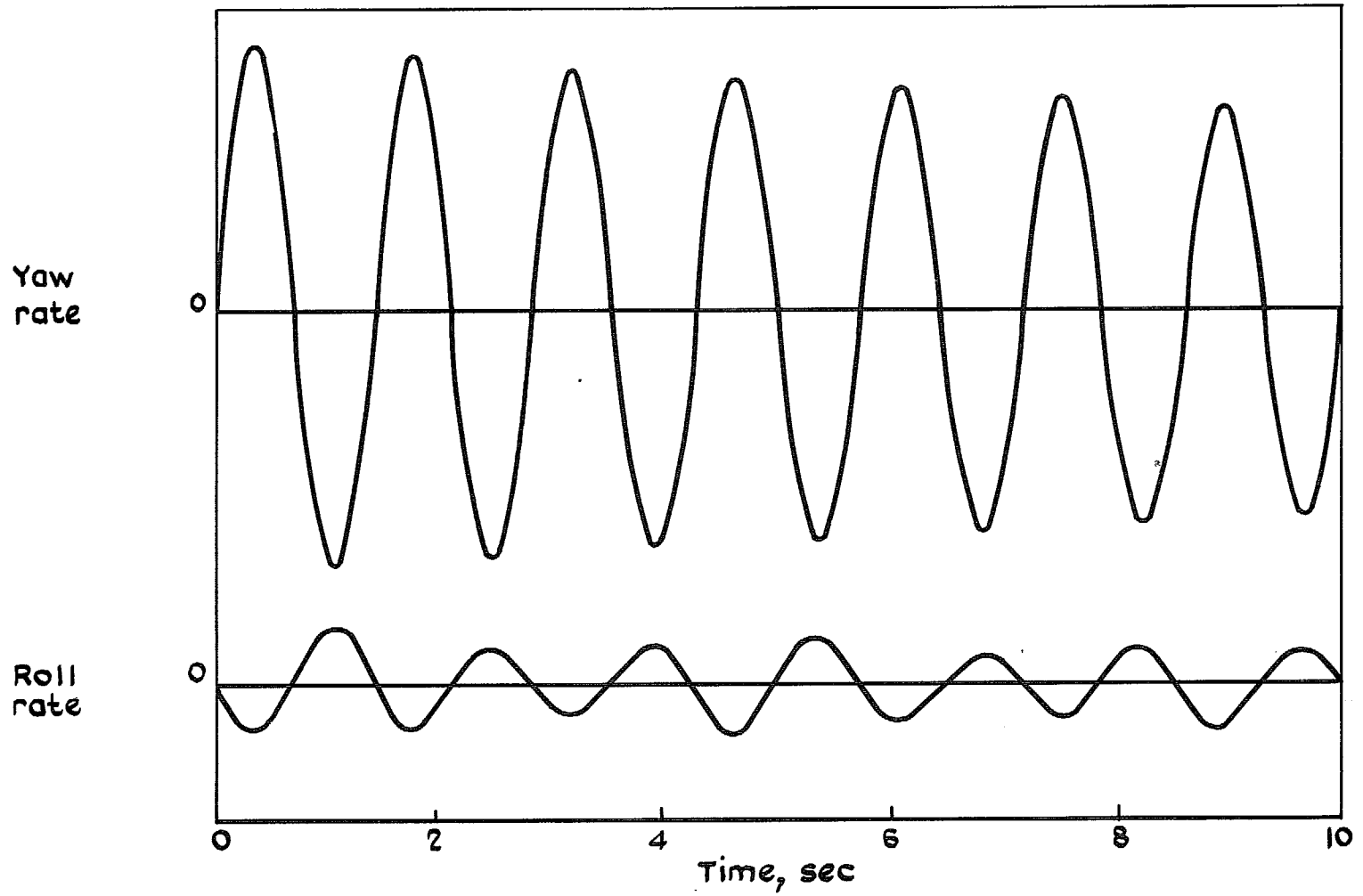
FIG. 14. Typical time histories and yaw and roll rates for oscillations of yaw inertia rig. (Nominal zero fuel, spring height 4, 4).
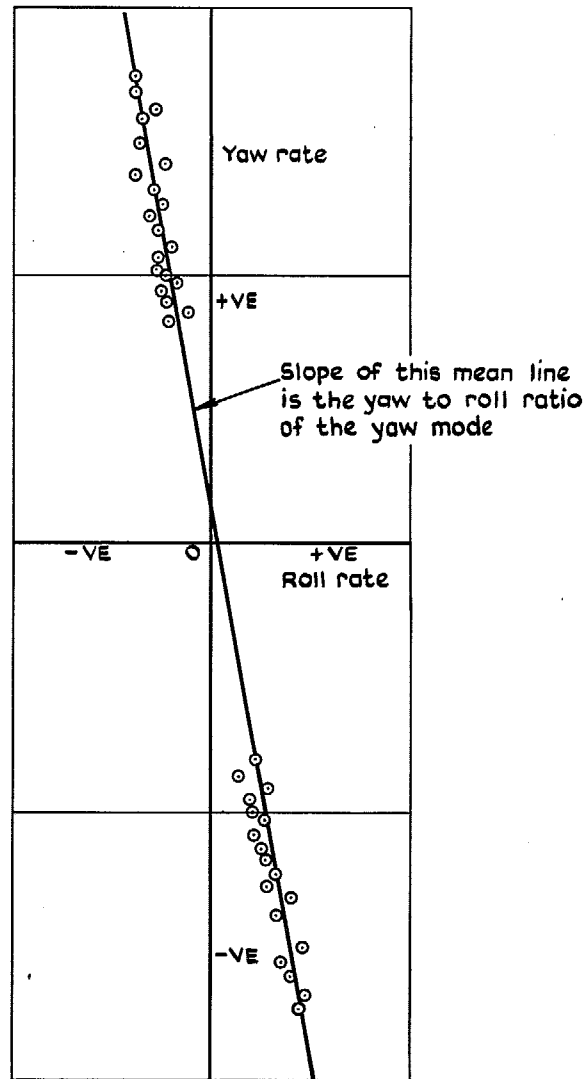
FIG. 15. Typical cross plot of roll and yaw rates
(nominal zero fuel case, spring height (4, 4).
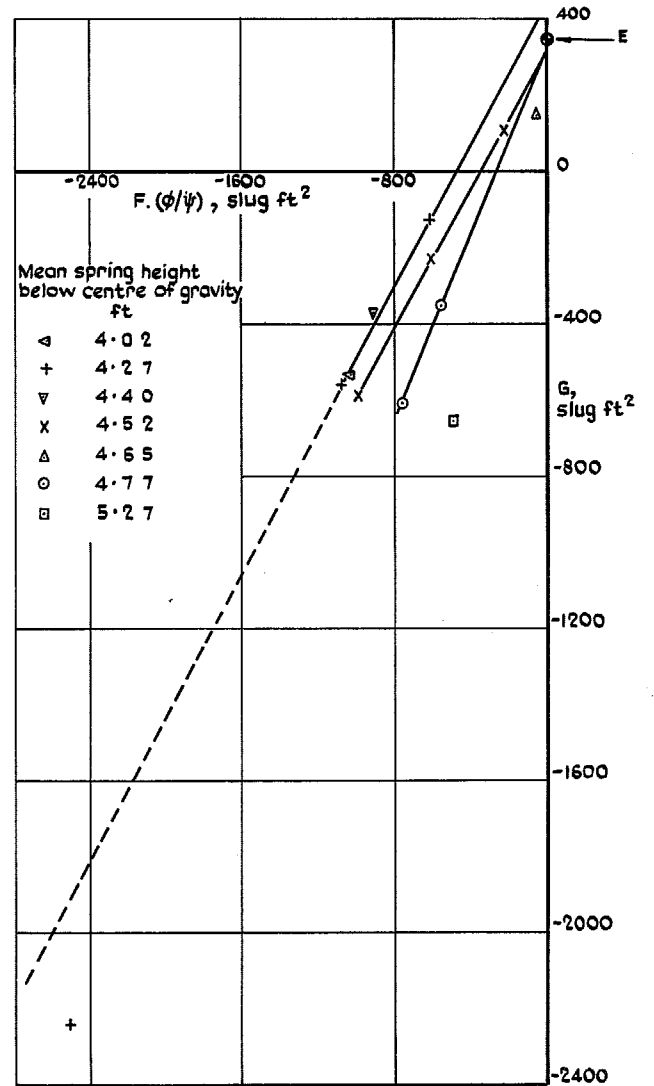
FIG. 16. Derivation of the product of inertia,
aircraft empty.
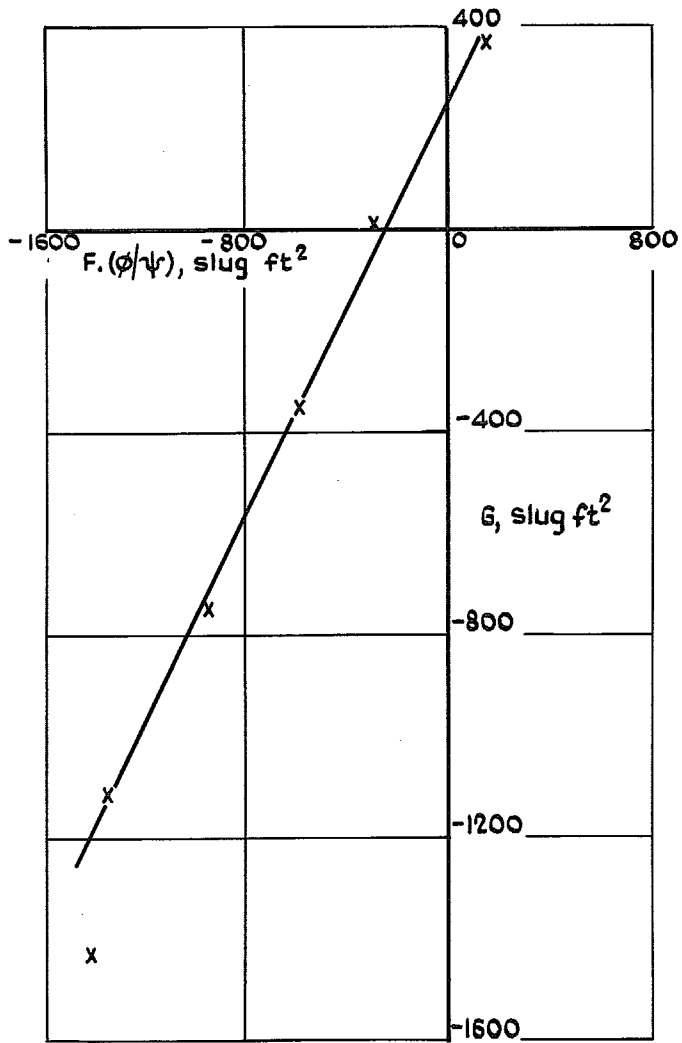
FIG. 17. Derivation of the product of inertia, full fuel.
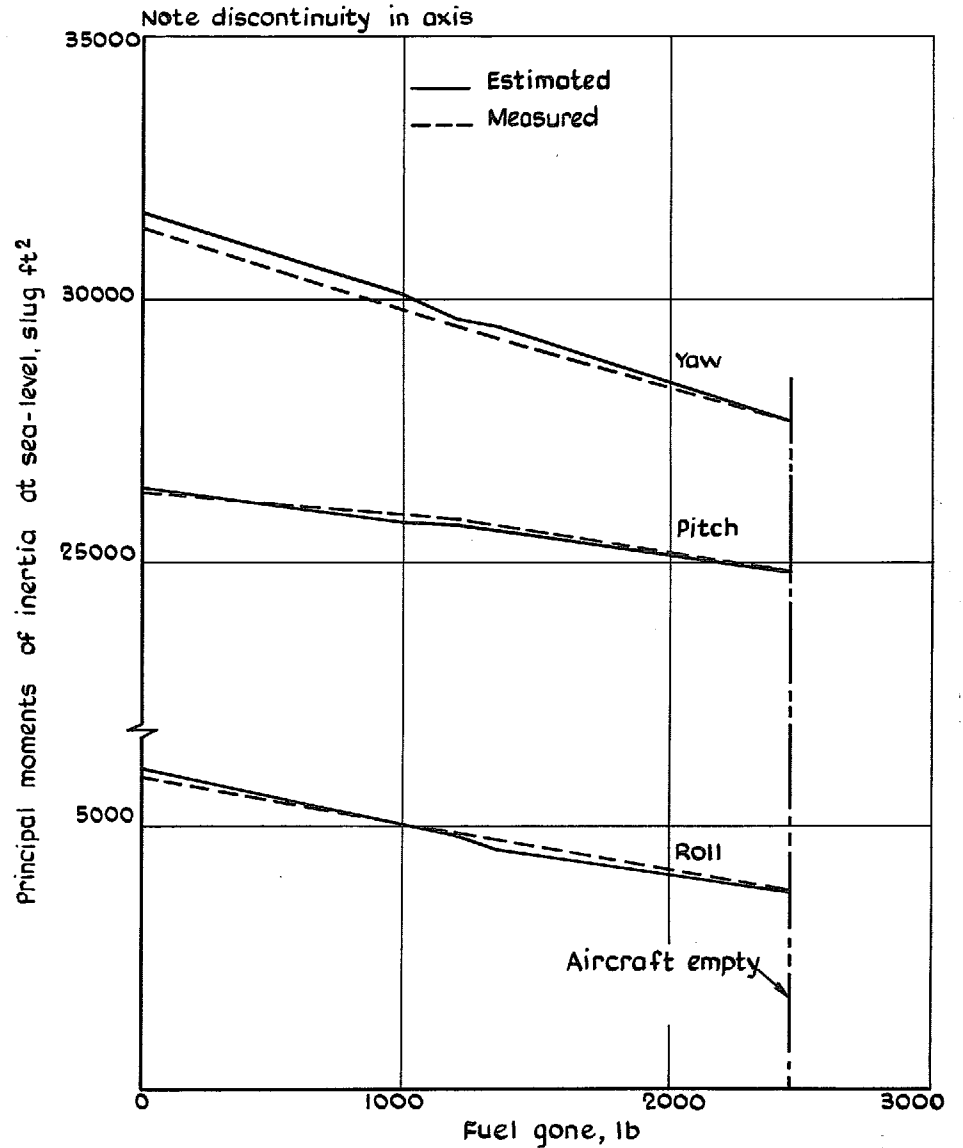
FIG. 18. Variation of principal moments of inertia with fuel state.
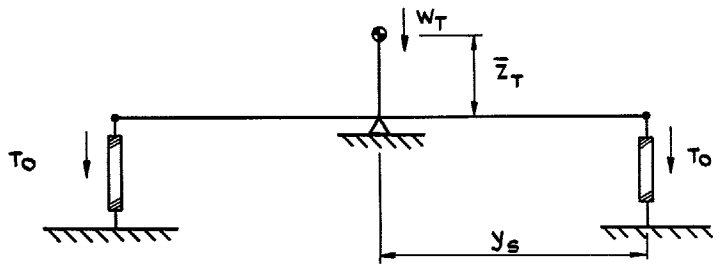
System in equilibrium
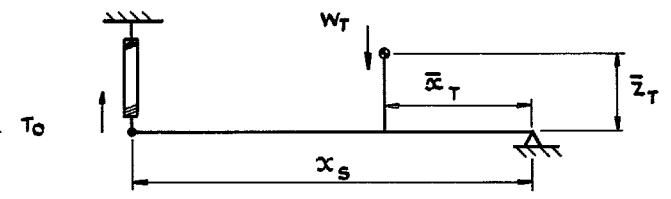
System in equilibrium
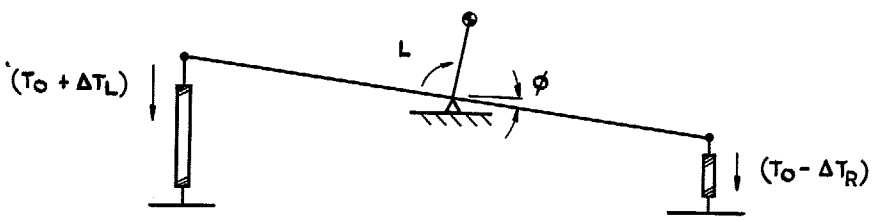
System displaced

System displaced
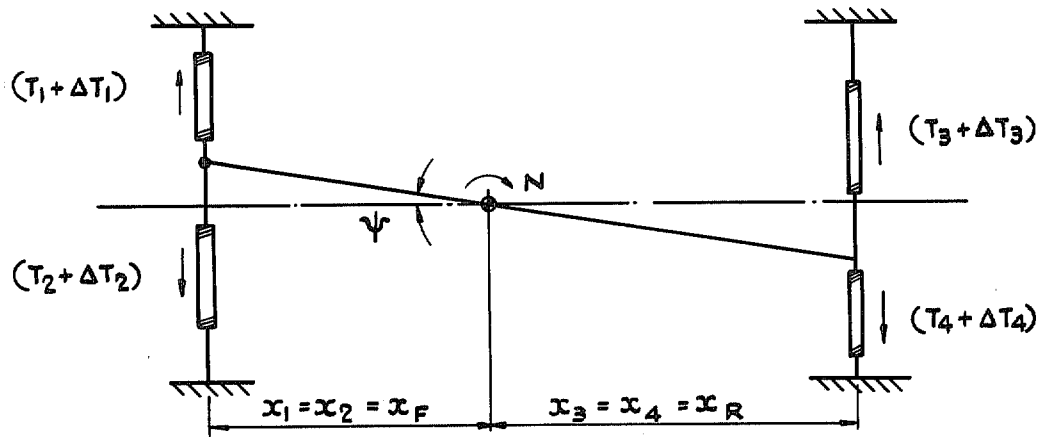
FIG. 19.   Roll inertia rig in diagrammatic form.

FIG. 20.   Pitch inertia rig in diagrammatic form.

h = a + b   q = h₁ + h₂
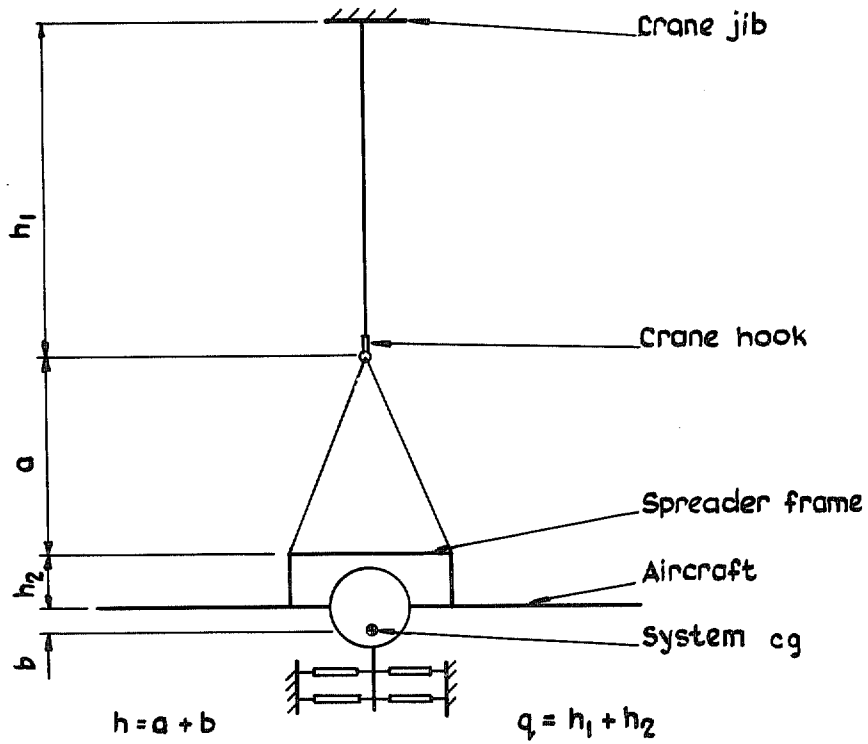
(a) Front elevation, system in equilibrium

(b) Plan, system displaced

FIG. 21 a & b.   Yaw inertia rig in diagrammatic form.